

Thompson Sampling Policy for Dynamic Participating Client Scenario in Federated Learning

Jialin Li, Tongjiang Yan, Yuanmeng Ding

Abstract—This article focuses on training a robust global model under the dynamic participating client scenario in federated learning (FL). Unlike the static FL scenario, this scenario emphasizes that new clients participate into modeling process at specific training round, a situation commonly encountered in Internet of Things (IoT) networks. Particularly, new participating clients may introduce irrelevant data (e.g., label noise, outliers, and distinct data distributions), posing the challenge for training a robust global model. To tackle this challenge, we introduce a novel FL framework called Fed-TS. This framework incorporates the Thompson sampling (TS) policy, a reinforcement learning (RL) approach, to enable biased client participation for both relevant and irrelevant clients during modeling process. Specifically, new clients can participate into modeling process based on their successful probability of causing “small path drift” in the global model. In addition, our framework employs an adaptive threshold using the K -means algorithm to assess “small path drift” in the global model. During the experiments, we investigate the impact of hyper-parameters on the performance of biased client participation for both relevant and irrelevant clients. Compared to other schemes or frameworks, our framework ensures a robust global model with high accuracy.

Index Terms—Dynamic participating client scenario, Federated learning, relevant clients, Thompson sampling policy

I. INTRODUCTION

WITH widespread adoption of smart devices and the rapid advancement of communication technology, data generated by multiple devices is growing explosively [1]. Based on privacy considerations, federated learning (FL) [2], [3] offers an efficient framework that enables multiple clients to collaboratively train a model without the need to share their local data. Currently, most FL-based frameworks have been proposed in the static scenario. These frameworks assume a fixed set of clients as the original client group before the initialization phase [4], [5]. Subsequently, the server selects a subset of clients from original client group and distributes the global model to the selected clients for collaborative modeling. However, as illustrated in Fig. 1, new clients can enter the FL system during modeling process. In Internet-of-Things (IoT) networks [6], [7], due to the client’s dynamic activities (such as client availability, network connectivity, user preference), it inevitably leads to an increase in the scale of the original client group. Furthermore, in Internet-of-Vehicles

This work was supported by Fundamental Research Funds for the Central Universities (23CX03003A), Shandong Provincial Natural Science Foundation of China (ZR2022MA061, ZR2023LZ013) and China Education Innovation Research Fund (2022BL027) (*Corresponding author: Tongjiang Yan*)

Jialin Li, Tongjiang Yan, and Yuanmeng Ding are with College of Sciences, China University of Petroleum (East China), Qingdao (e-mail: ljl19960221@163.com, yantoji@163.com, dingyuanmeng123@163.com)

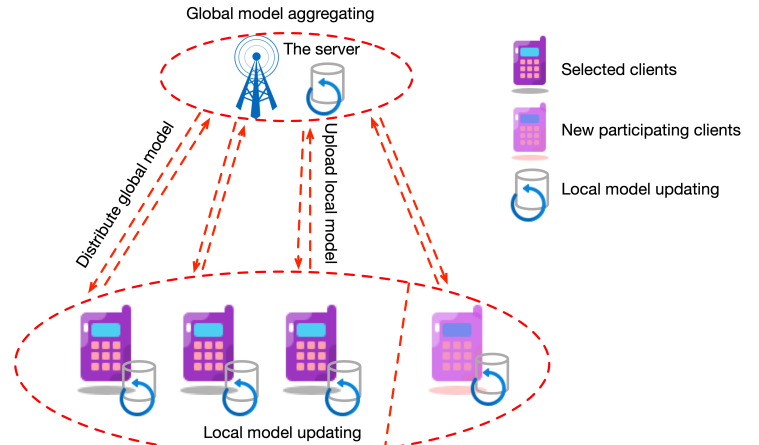


Fig. 1. The dynamic participating client scenario in FL.

(IoV) networks [8], vehicle activities are more dynamic, which means that vehicles are constantly moving while generating a large amount of real-time data. This dynamism also leads to a dynamic expansion of the original vehicle group. In these two scenarios, the static FL-based frameworks may not be able to adapt to the dynamic client participation.

The potential data quality of new participating client is an important factor in FL. From the perspective of enhancing model’s stability, Nagalappatti et al. [9] proposed two client concepts: **Relevant clients** and **Irrelevant clients**. A client called an irrelevant client if the update it shares leads to poor model performance (e.g., the convergence speed and test accuracy) of the global model. Typically, the irrelevant client often possess low-quality data, which may include label noise [10], outliers [11], and data that do not conform to the target distribution [12]. Therefore, in the scenario where irrelevant clients participate dynamically, training a robust global model becomes a challenge.

To develop a robust global model, some efforts have been proposed to address the issue of data heterogeneity, including: enforcing regularization in local optimization [13], [15], improving the model aggregation scheme [14], [16], and introducing personalization technique [17], [18]. However, these efforts are based on a fixed original client group assumption, neglecting the impact of new participating clients. The FedREM framework [19] has been proposed to address the issue of data heterogeneity under the participating client scenario. The core idea is to guide new clients to fit into the global training through retraining and matching the learnable parameters of batch normalization (BN) layers [20]. However, such framework is limited to convolutional neural network

(CNN) models [21] that contain BN layers.

In addition, among irrelevant clients, there are malicious ones [22] that can manipulate their local datasets or submit incorrect gradient information, which also undermine the robustness of the global model. The aforementioned frameworks do not take the malicious attacks into account. A notable exception is that the FedCHR framework [23] has also focused on the issue of defending against malicious client attacks under the dynamic participating client scenario. This framework identifies malicious clients by comparing their gradients to those of benign clients. However, from a similarity perspective, this approach relies heavily on the extreme diversity of local data and often struggles in scenarios of limited diversity of local data.

Furthermore, some efforts focus on developing client participation schemes. Most FL frameworks have employed the unbiased participation scheme, specifically a random scheme [24], wherein each client has an equal probability of participating into modeling process. For the biased schemes, existing FL frameworks have utilized additional prior knowledge to enhance client participation, considering factors such as training loss [25], training efficiency [26], and computational capabilities [27], [28]. However, these schemes do not consider the participating client scenario, and there is no guarantee that they can achieve biased participation for both relevant and irrelevant clients during modeling process.

In this paper, we propose a novel client participation scheme based on Thompson sampling (TS) policy, which can achieve biased client participation for both relevant and irrelevant clients. Specifically, the participation scheme will be reformulated as a combinatorial multi-armed bandit (CMAB) problem [29], where the goal is to select the optimal subset from new participating clients at each round. In contrast to the upper confidence bound (UCB) policy used in [30], [31], and [32] to address the CMAB problem, our framework employs the Thompson sampling (TS) policy [33], which facilitates probabilistic exploration of the **unknown characteristic** for the relevant clients. Here, the successful probability of causing “small path drift” in the global model (described by a binomial distribution) serves as the **unknown characteristic** of the relevant client. The contributions of this paper are summarized as follows:

- To obtain the robust global model under the dynamic participating client scenario, we propose a novel FL framework, named Fed-TS, which can achieve biased client participation for both relevant and irrelevant clients.
- Especially, during the client participation phase, the multiple-play Thompson sampling (MP-TS) algorithm is utilized to complete the top- p clients selection. To adapt the MP-TS algorithm to real-world scenarios, a client participation size strategy is also proposed. During the distribution updating phase, the successful probability of facilitating “small path drift” in the global model is used to update the posterior Beta distribution of the selected clients. In addition, an adaptive threshold using the K -means algorithm is also employed to assess “small path drift” in the global model.

- The regret bound of training interval between two selections of the relevant client is provided, indicating that our framework can achieve biased client participation. Meanwhile, the convergence guarantee for the global model is also provided.
- For our experiments, we construct three dynamic participating client scenarios, i.e., label-flipping attack, data heterogeneity and model-poisoning attack. Firstly, we investigate the impact of hyper-parameters on the performance of biased participation for both relevant and irrelevant clients. Furthermore, we compare our framework with other schemes or frameworks, and the results show that our proposed framework trains a robust global model with high accuracy. Finally, we test the scalability of our framework.

II. RELATED WORK

A. FL framework in solving the clients with irrelevant data

1) *Data heterogeneity*: To alleviate the irrelevant clients with data heterogeneity, many frameworks have been proposed. The FedProx framework [13] adds a proximal term into the objective function to constrain the distance to the global model. The FedBN framework [14] proposes an effective method using local batch normalization to alleviate the data heterogeneity before aggregating the global model. The FedDyn framework [15] provides a dynamic regularizer for each device to limit the global and local models. The Scaffold [16] framework uses the control variance that can correct the path drift in its local update to solve the data heterogeneity. The FedGen framework [17] proposes a knowledge distillation approach to address data heterogeneity, in which the server trains a lightweight model and transfers its knowledge to clients, regulating local training using the learned knowledge. The paper [34] proposes the efficient FL framework using ADAM and YOGI optimizers for data heterogeneity problem. The GOFL framework [35] incorporates the federated gradient normalization (FGN) technique to mitigate the path-drift impact caused by clients’ data heterogeneity. These frameworks cannot consider the dynamic participation scenario. The FedREM framework [19] considers the scenario of client participation, but it has significant model limitations.

2) *Malicious robustness*: Recently, Byzantine-robust techniques [36] have been considered to defend against malicious attacks. For example, the MKrum method [37] selects several local models with smaller distances and averages them to form the global model. The Median method [38] obtains the global parameters by selecting the median of all local model parameters at each position. The paper [39] proposes a privacy-preserving framework achieves Bayesian robustness through cosine distance scoring and dynamic model selection. Similar to the MKrum method, the FedCHR framework [23] uses the cosine similarity to measure the distance between the global model and the local models, allowing new clients with small cosine similarity. However, in real-world scenarios, it is difficult to determine the number of malicious clients, which presents a challenge for this framework.

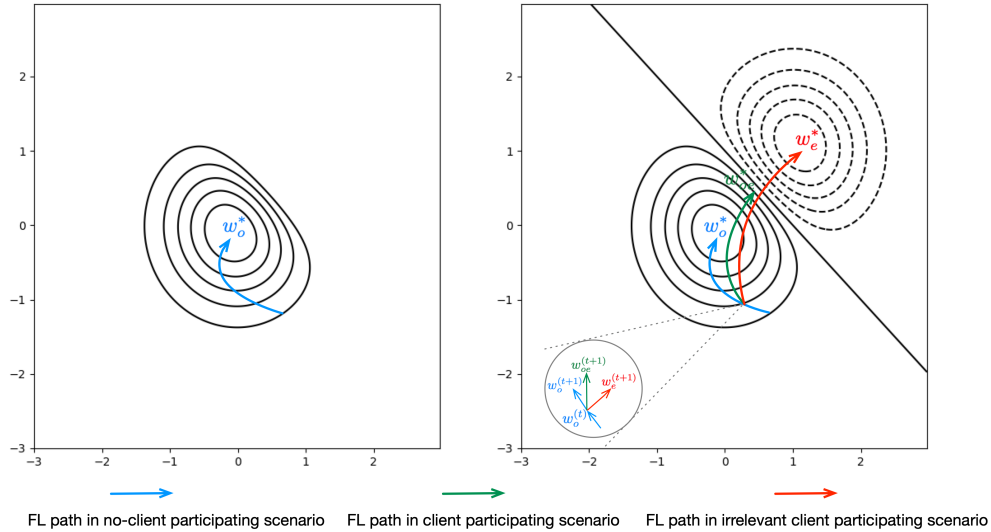


Fig. 2. The illustration of path drift in the global model with two features, applies to no-client participation and dynamic client participation scenarios.

B. FL framework based on TS strategy

Recently, some works have considered combining the FL framework with TS. The FedRTS framework [40] is proposed to address the challenge of model sparsification in FL by integrating a TS-based method to achieve an efficient sparse model. The paper [40] tackles the issue of adversarial attacks in vertical federated learning (VFL), proposing the TS method combined with the Empirical Maximum Reward (E-TS) algorithm to counter these attacks. Meanwhile, the paper [42] introduces the FTS framework, which is based on TS, to minimize the number of exchanged parameters. Unlike these works, this paper focuses on the dynamic participating client scenario in FL. The Fed-TS framework uses the TS policy to achieve biased client participation for both relevant and irrelevant clients, which can solve this challenge.

III. DYNAMIC PARTICIPATING CLIENT SCENARIO

A. The Optimization Model

Consider a network including one server and multiple clients. Let $\mathcal{I}_o = \{c_{o,1}, c_{o,2}, \dots, c_{o,N_o}\}$ denote the set of original client group, and each client can train the global model. In this scenario, the global loss is formulated as follows:

$$F_o(\mathbf{w}) = \frac{1}{N_o} \sum_{i_o \in \mathcal{I}_o} f_{i_o}(\mathbf{w}), \quad (1)$$

where \mathbf{w} and f_{i_o} represent the model parameter and local loss, respectively. According to the model aggregation rule, the optimal solution to (1) can be expressed as:

$$\mathbf{w}_o^{(t)} = \frac{1}{|\mathcal{S}_o^t|} \sum_{i_o \in \mathcal{S}_o^t} \mathbf{w}_{i_o}^{(t)}, \quad (2)$$

where $\mathbf{w}_o^{(t)}$ and $\mathbf{w}_{i_o}^{(t)}$ are the global model and the local model at round t , respectively. In addition, \mathcal{S}_o^t represents the set of sampling clients from group \mathcal{I}_o with a size of $|\mathcal{S}_o^t|$.

Next, we consider the dynamic participating client scenario. At round t_0 , the participation client group $\mathcal{I}_e = \{c_{e,1}, c_{e,2}, \dots, c_{e,N_e}\}$ will come into group \mathcal{I}_o . The global loss is formulated as follows:

$$F(\mathbf{w}) = \frac{1}{N} \sum_{i_o \in \mathcal{I}_o} f_{i_o}(\mathbf{w}) + \frac{1}{N} \sum_{i_e \in \mathcal{I}_e} f_{i_e}(\mathbf{w}), \quad (3)$$

where N is equal to $N_o + N_e$, and $f_{i_e}(\mathbf{w})$ represents the local loss from group \mathcal{I}_e . After the t_0 -th round, the global model $\mathbf{w}_{oe}^{(t)}$ can be aggregated as follows:

$$\mathbf{w}_{oe}^{(t)} = \underbrace{\frac{1}{|\mathcal{S}_{oe}^t|} \sum_{i_o \in \mathcal{S}_o^t} \mathbf{w}_{i_o}^{(t)}}_{\text{basic part}} + \underbrace{\frac{1}{|\mathcal{S}_{oe}^t|} \sum_{i_e \in \mathcal{S}_e^t} \mathbf{w}_{i_e}^{(t)}}_{\text{participating part}}, \quad (4)$$

where $|\mathcal{S}_{oe}^t| = |\mathcal{S}_o^t| + |\mathcal{S}_e^t|$, and $\mathbf{w}_{i_e}^{(t)}$ represent the local model from group \mathcal{I}_e . Different from Eq. (2), it can be noted that the global model will be divided into two parts: the basic part and participating part. Intuitively, the participating part introduces the diversity between $\mathbf{w}_o^{(t)}$ and $\mathbf{w}_{oe}^{(t)}$.

B. Path Drift in the Global Model

In this subsection, we describe the diversity between $\mathbf{w}_o^{(t)}$ and $\mathbf{w}_{oe}^{(t)}$. According to [16], path drift frequently occurs in scenarios with data heterogeneity, which negatively impacts the robustness of the global model. In this paper, we utilize this concept to analyze the dynamic participating client scenario.

Fig. 2 illustrates the phenomenon of path drift under the dynamic participating client scenario. In the scenario with no clients participating, the FL path (indicated by the blue line) converges to a global optimum \mathbf{w}_o^* , influenced by the data distribution \mathcal{V}_o . At round t_0 , new clients will come into group \mathcal{I}_o . Especially, the introduction of irrelevant clients' data distributions \mathcal{V}_e leads to a shift in the global optimum from

\mathbf{w}_o^* to \mathbf{w}_{oe}^* . Consequently, the FL path of the global model transitions from $\mathbf{w}_o^{(t)}$ to \mathbf{w}_{oe}^* (indicated by the green line), rather than from $\mathbf{w}_o^{(t)}$ to \mathbf{w}_o^* (indicated by blue line). Notably, at round t_0 , influenced by the dynamic part $\mathbf{w}_e^{(t)}$, the FL path shifts towards $\mathbf{w}_{oe}^{(t+1)}$.

IV. PROBLEM FORMULATION

A. Combinatorial Multi-armed Bandit Problem

At round t , we view the client participation group \mathcal{I}_e as a slot machine with N_e clients, where each client i_e yields a reward $X_{i_e}^t$. The reward follow an unknown distribution with mean u_{i_e} . Let $\mathcal{S}_p^t (\mathcal{S}_p^t \subseteq \mathcal{I}_e)$ denote the set of selected clients with $|\mathcal{S}_p^t| \geq 1$. Over a total of T rounds, the \mathcal{S}_p^t from group \mathcal{I}_e is determined over the rounds $t = \{t_0, t_0 + 1, \dots, T\}$.

B. Thompson sampling policy for the CMAB problem

Firstly, the general Thompson sampling (TS) policy for solving the CMAB problem is reviewed. We also provide the motivation for adopting the TS policy for biased client participation.

Before introducing the general TS policy, an oracle function $Oracle(\Theta)$ [43], [44] is introduced, that takes a vector of parameters $\Theta = [\theta_1^t, \dots, \theta_{N_e}^t]$ as input, and outputs the subset \mathcal{S}_p^t . The general TS policy is described in Algorithm 1. Initially, each client i_e is associated with prior Beta distribution $\beta(1, 1)$. At round t , all clients draw a sample $\theta_{i_e}^t$ from corresponding posterior Beta distribution $\beta(s_{i_e}^t, f_{i_e}^t)$. Here, $s_{i_e}^t$ and $f_{i_e}^t$ represent the number of successful and failed explorations, respectively. According to the rule of oracle function, we can get the subset \mathcal{S}_p^t and corresponding rewards $\{X_{i_e}^t\}_{i_e \in \mathcal{S}_p^t}$. Following the updating procedure (see Algorithm 2), the posterior Beta distribution is updated as $\beta(s_{i_e}^t + k, f_{i_e}^t + 1 - k)$ after observing $\{X_{i_e}^t\}_{i_e \in \mathcal{S}_p^t}$, where k is the Bernoulli variable.

Algorithm 1: TS policy for the CMAB problem

```

For the participating client  $i_e$ , let  $s_{i_e}^0 = f_{i_e}^0 = 1$ 
for  $t = t_0, t_0 + 1, \dots, T$  do
    For new clients  $i_e$ , draw a sample  $\theta_{i_e}(t)$  from Beta
        distribution  $\beta(s_{i_e}^t, f_{i_e}^t)$  to obtain  $\Theta^t$ 
    Select  $\mathcal{S}_p^t$  according to  $Oracle(\Theta^t)$ , and get the
        rewards  $\{X_{i_e}^t\}_{i_e \in \mathcal{S}_p^t}$ 
    Update  $\{s_{i_e}^t, f_{i_e}^t\}_{i_e \in \mathcal{S}_p^t}$  based on  $\{X_{i_e}^t\}_{i_e \in \mathcal{S}_p^t}$ 
end
```

Algorithm 2: Updating procedure

```

Input:  $\{s_{i_e}^t, f_{i_e}^t\}_{i_e \in \mathcal{S}_p^t}, \{X_{i_e}^t\}_{i_e \in \mathcal{S}_p^t}$ 
Output: updated  $\{s_{i_e}^t, f_{i_e}^t\}_{i_e \in \mathcal{S}_p^t}$ 
for  $i_e \in \mathcal{S}_p(t)$  do
     $k \leftarrow 1$  with probability  $P(X_{i_e}^t)$ , 0 with probability
         $1 - P(X_{i_e}^t)$ 
     $s_{i_e}^t \leftarrow s_{i_e}^t + k; f_{i_e}^t \leftarrow f_{i_e}^t + 1 - k$ 
end
```

Motivation: The general TS policy is a natural Bayesian probability algorithm. The basic idea is to select the optimal subset \mathcal{S}_p^* according to its sample from posterior Beta distribution. For instance, assume that $Oracle(\Theta) = \arg \max_{i_e} (\Theta^t)$, i.e., selecting the client i_e with highest sample at each round. Initially, the Beta distribution $\beta(1, 1)$ is equivalent to the uniform distribution $[0, 1]$, meaning that drawing a client's $\theta_{i_e}^t$ can be viewed as a random sampling process. As a result, each client has the equal probability of participating into original client group. As T increases, the client i_e , characterized by a right-skewed Beta distribution, becomes more likely to obtain a high sample, thereby increasing the probability of coming into the original client group. To achieve progressively biased participation among new participating clients, we incorporate TS policy into the proposed framework.

V. THE PROPOSED FRAMEWORK

Our framework contains two phases: client participation phase and distribution updating phase. During the client participation phase, the multiple-play Thompson sampling (MP-TS) algorithm [43] is utilized to select the subset \mathcal{S}_p^t at each round. During the distribution updating phase, each selected client updates its corresponding posterior Beta distribution based on the outcomes of successful or failed explorations.

A. Client Participation Phase

As mentioned in the TS policy, let denote the set of clients' Beta distributions as $\mathcal{B}^t = [B_1^t, \dots, B_{i_e}^t, \dots, B_{N_e}^t]$ for group \mathcal{I}_e , where $B_{i_e}^t = \beta(s_{i_e}^t, f_{i_e}^t)$. Correspondingly, $\Theta^t = [\theta_1^t, \dots, \theta_{i_e}^t, \dots, \theta_{N_e}^t]$ denotes the vector of sample drawing from \mathcal{B}^t . For the formulation of oracle function, the MP-TS algorithm [43] is considered as follows:

$$Oracle(\Theta^t) = \underbrace{\mathcal{M}(\Theta^t; \theta_{[p]}^t)}_{\mathcal{S}_p^t}, \quad (5)$$

where $\theta_{[p]}^t$ denotes the p -th largest sample, p represents the client participation size, and $\mathcal{M}(\cdot)$ is the mapping function that selects the clients with $\theta_{i_e}^t \geq \theta_{[p]}^t$. Therefore, the top- p clients are selected as the subset \mathcal{S}_p^t . In practical scenario, the true client participation size \tilde{p} of relevant clients among new participants is unknown to us. In this paper, we investigate the relationship between the set client participation size p and the true client participation size \tilde{p} .

- Case 1: The client participation size p equals true client participation size \tilde{p} .
- Case 2: The client participation size p exceeds true client participation size \tilde{p} .

Remark: Case 1 corresponds to the scenario where we already know the size of relevant clients from new participating clients. In this case, we provided the theoretical analysis (see Subsection VI-A). Case 2, on the other hand, involves a scenario where the true size of relevant clients from new participating clients is unknown. To obtain the true client participation size, the client participation size search strategy is proposed.

Let $\mathcal{K}^t = \{sk_1^t, \dots, sk_{i_e}^t, \dots, sk_{N_e}^t\}$ denote the set of clients' skewness values, where $sk_{i_e}^t$ is formulated as follows:

$$sk_{i_e}^t = \frac{2(s_{i_e}^t - f_{i_e}^t)\sqrt{s_{i_e}^t + f_{i_e}^t + 1}}{(s_{i_e}^t + f_{i_e}^t)(s_{i_e}^t + f_{i_e}^t + 1)}.$$

Suppose that $l^t = \{l_1^t, \dots, l_{i_e}^t, \dots, l_{N_e}^t\}$ is the set of selection rounds for the clients. In our paper, the selection rounds can be viewed as a cumulative metric, reflecting the total number of rounds in which a client has been selected throughout the training process. If a client is selected by the server 25 times during the total training rounds, then the number of selection rounds for that client is 25. Then, the strategy is summarized in Algorithm 3.

Algorithm 3: Client participation size search strategy

Input: $p, L, \mathcal{B}^t, l^t, \mathcal{K}^t$
Output: Updated p
if $\forall i_e \in l^t, l_{i_e}^t > L$ **do**
 Search the set $\mathcal{K}_o^t = \{i_e \in \mathcal{K}^t | sk_{i_e} < 0\}$
 Update $p = N_e - |\mathcal{K}_o^t|$
end

Specifically, the client participation size search strategy is based on the skewness of updating Beta distribution to search the true client participation size \tilde{p} . The motivation of this strategy comes from Lemma 1, which states that when irrelevant clients reach the warm-up rounds (see Definition 2), their corresponding Beta distribution becomes stable. Accordingly, irrelevant clients correspond to a right-skewed Beta distribution, while relevant clients correspond to a left-skewed distribution. The client participation size search strategy has two hyper-meters: the original client participation size p and the selected threshold L . In Subsection VII-C, the experimental analysis and practical guidance are summarized.

B. Distribution Updating Phase

During this phase, our framework focuses on updating the successful or failed explorations for the selected clients. Here, the Binomial distribution is employed to characterize the client's reward $X_{i_e}^t$ as follows:

$$P(X_{i_e}^t = k) = \begin{cases} u_{i_e}, & \text{if } k = 1, \\ 1 - u_{i_e}, & \text{if } k = 0, \end{cases} \quad (6)$$

where u_{i_e} represents the successful probability of the **unknown characteristic**. If the reward $X_{i_e}^t$ is equal to 1, the client performs a successful exploration, otherwise, it is a failed exploration.

Inspired by the fact that the participating irrelevant client can lead to severe path drift, the ability of causing "small path drift" in the global model serves as the **unknown characteristic**. Mathematically, the ability of causing "small path drift" in the global model is formulated as follows:

$$\begin{cases} k = 1, & \text{if } 0 \leq \|\mathbf{w}_{oi_e}^{(t)} - \mathbf{w}_o^{(t)}\|^2 \leq \alpha^{(t)}, \\ k = 0, & \text{if otherwise,} \end{cases} \quad (7)$$

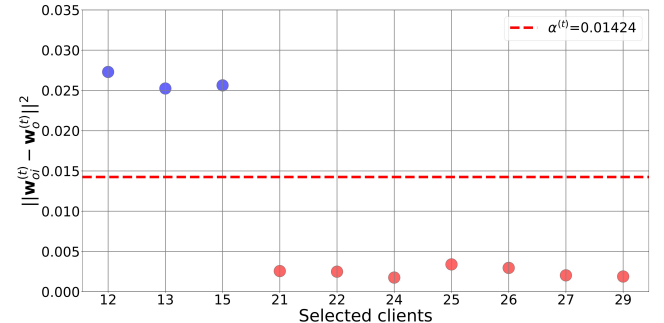


Fig. 3. The illustration of the adaptive threshold $\alpha^{(t)}$. Furthermore, the irrelevant client indexes with $\{12, 13, 15\}$ and, the relevant client indexes with $\{21, 22, 24, 25, 26, 27, 29\}$.

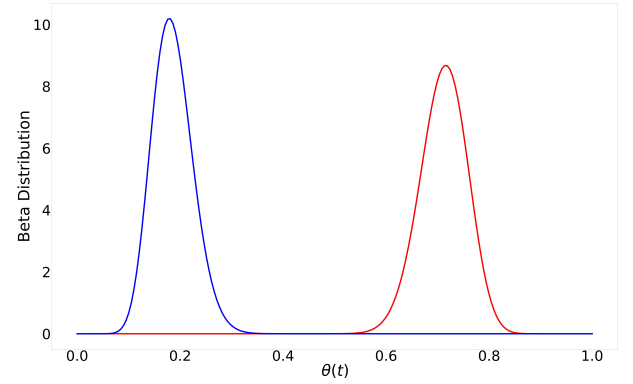


Fig. 4. The Beta distribution of the clients at the 100-th round in the CIFAR-10 dataset. (1) Blue line represents the irrelevant client with $\beta(18, 79)$ (2) Red line represents the relevant client with $\beta(78, 15)$.

where $\alpha^{(t)}$ represents the adaptive threshold to assess the "small path drift", and the L-2 norm is utilized as the measurement for $\mathbf{w}_{oi_e}^{(t)}$ and $\mathbf{w}_o^{(t)}$. In addition, the virtual global model $\mathbf{w}_{oi_e}^{(t)}$ is also introduced as follows:

$$\mathbf{w}_{oi_e}^{(t)} = \frac{\sum_{i_o \in S_o^t} \mathbf{w}_{i_o}^{(t)} + \varepsilon \mathbf{w}_{i_e}^{(t)}}{|S_o^t| + \varepsilon}, \quad (8)$$

where $\varepsilon (\varepsilon \in \mathbb{R}^+)$ represents the aggregation weight for the client i_e with $i_e \in S_p^t$.

Here, we construct $\|\mathbf{w}_{oi_e}^{(t)} - \mathbf{w}_o^{(t)}\|^2$ to measure the drift of the client i_e on the original FL path. Eq. (8) also introduces the aggregation weight ε to improve the client's contribution. When ε is set to 1, we will get a sample average aggregation for the client i_e . We introduce the hyper-parameter ε to enhance the aggregation contribution of a participation client, improving the successful and failed explorations with our framework. The impact of hyper-parameter ε is present in Subsection VII-D.

C. The Adaptive Threshold Using the K-means Algorithm

Our framework computes the $\alpha^{(t)}$ that can distinguish the relevant client (high number of successful explorations) and

irrelevant client (low number of successful explorations). Since $\|\mathbf{w}_{oe} - \mathbf{w}_o\|^2$ reflects the diversity of a participating client, we focus on the client with high $\|\mathbf{w}_{oe} - \mathbf{w}_o\|^2$. Then, the problem can be summarized as follows: how to set the $\alpha^{(t)}$ to find the clients with high $\|\mathbf{w}_{ie} - \mathbf{w}_o\|^2$ from the set $\mathcal{W}^{(t)} = \{\Delta \mathbf{w}_{ie}^{(t)} : \|\mathbf{w}_{oe}^{(t)} - \mathbf{w}_o^{(t)}\|^2 \mid i_e \in \mathcal{S}_p^t\}$. This problem can be transformed into an unsupervised problem. For that, we implement a binary classification scheme using K -means algorithm [45] in which clusters "1" and "0" represent successful exploration and failed exploration, respectively.

Let $A = \{\alpha_0^{(t)}, \alpha_1^{(t)}\}$ represent two centroids. The objective function is $J(\mathcal{W}^{(t)}) = \sum_{i_e \in \mathcal{S}_p^t} \sum_{j \in \{0,1\}} z_{ie,j} \|\Delta \mathbf{w}_{ie}^{(t)} - a_j\|^2$, where $z_{ie,j}$ is a binary variable indicating whether $\Delta \mathbf{w}_{ie}^{(t)}$ belongs to the cluster j ($j = 0, 1$). The centroids from A are updated at each round, i.e.,

$$\alpha_{\{j|j=0,1\}}^{(t)} = \frac{\sum_{i_e \in \mathcal{S}_p^t} z_{ie,j} \Delta \mathbf{w}_{ie}^{(t)}}{\sum_{i_e \in \mathcal{S}_p^t} z_{ie,j}}. \quad (9)$$

After that, the following adaptive threshold $\alpha^{(t)}$ is introduced as follows:

$$\alpha^{(t)} = \frac{\alpha_0^{(t)} + \alpha_1^{(t)}}{2}. \quad (10)$$

At the t_0 -th round, the server randomly initializes two centroids, i.e., $\alpha_0^{(t_0)}$ and $\alpha_1^{(t_0)}$. After receiving the set $\mathcal{W}^{(t)}$, it updates the centroids, and the new centroids will be used for the next initialization.

Remark: Fig. 3 illustrates the process of the adaptive threshold $\alpha^{(t)}$. By calculating the median between the two centroids, we can effectively categorize the selected clients into two clusters: successful exploration and failed exploration. On the other hand, our framework allows clients to perform multiple explorations to update their corresponding Beta distributions. As shown in Fig. 4, an incorrect classification during one exploration does not affect the overall skewness of its Beta distribution.

D. Overflow of the Proposed Framework

In this part, we incorporate the client participation phase and distribution updating phase into the Fed-TS framework. In detail, the specific steps are summarized in algorithm 4 as follows:

- Step 1: The server initializes the set \mathcal{B}^{t_0} of all participating clients. Correspondingly, each client's Beta distribution $B_{ie}^{t_0}$ is initialized as $\beta(s_{ie}^{t_0} = 1, f_{ie}^{t_0} = 1)$.
- Step 2: The server sets the p_o and p to select the clients from the groups \mathcal{I}_o and \mathcal{I}_e , respectively. Similar to most FL frameworks [13], [24], for the group \mathcal{I}_o , a random scheme is employed to obtain the subset \mathcal{S}_o^t . According to Eq. (5), the server obtains subset \mathcal{S}_p^t from group \mathcal{I}_e .
- Step 3: All selected clients compute their local models and send them to the server.
- Step 4: The server computes the adaptive threshold $\alpha^{(t)}$, global model $\mathbf{w}_o^{(t)}$, and virtual global model $\mathbf{w}_{oe}^{(t)}$. By computing $\|\mathbf{w}_{oe}^{(t)} - \mathbf{w}_o^{(t)}\|^2$, the server updates $\{s_{ie}^{t}, f_{ie}^{t}\}$ of Beta distribution for the selected clients. Finally, the

server gets the global model $\mathbf{w}_{oe}^{(t)}$, and the server performs the client participation size search strategy.

Algorithm 4: The Fed-TS framework

```

for  $t = t_0, \dots, T$  do
    if  $t = t_0$  then
        | The server initializes the set  $\mathcal{B}^{(t_0)}$  of new
        | participating clients with  $\beta(s_i^{t_0} = 1, f_i^{t_0} = 1)$ .
    end

    Client Selection Phase:
        The server selects  $\mathcal{S}_o^t$  from group  $\mathcal{I}_o$  using the
        random scheme.
        The server selects  $\mathcal{S}_p^t$  from group  $\mathcal{I}_e$  using Eq.
        (5).
        for  $i_o \in \mathcal{S}_o^t$  do
            | Each client computes  $\mathbf{w}_{i_o}^{(t)}$ , and sends it to the
            | server.
        end
        for  $i_e \in \mathcal{S}_p^t$  do
            | Each client computes  $\mathbf{w}_{i_e}^{(t)}$ , and sends it to the
            | server.
        end

    Distribution Updating Phase:
        The server updates the Beta distribution for the
        selected clients from  $\mathcal{S}_p^t$  using Eqs. (7) and (10).
        The server computes global model  $\mathbf{w}_{oe}^{(t)}$ , and
        distributes it to all clients for next initialization.
        The server performs the client participation size
        search strategy in Algorithm 3.
    end

```

The analysis of time complexity and communication complexity is provided as follows:

Time complexity: The server needs to obtain all client's sample form \mathcal{B}^t with complexity of $\mathcal{O}(N_e)$. According to the MP-TS algorithm, the server also participates the top- p large-sample clients into modeling process. This process uses a sort algorithm with time complexity of $\mathcal{O}(N_e \log(N_e))$. During the distribution updating phase, the server needs to assess "small path drift" in the global model based on the K -means algorithm for the selected clients. This process has time complexity of $\mathcal{O}(\mathcal{Q}|\mathcal{S}_p^t| + |\mathcal{S}_p^t|)$, where \mathcal{Q} represents the model dimension. In Algorithm 3, this strategy has time complexity of $\mathcal{O}(N_e)$. Finally, the server aggregates the global model with time complexity of $\mathcal{O}(\mathcal{Q}|\mathcal{S}_o^t| + \mathcal{Q}|\mathcal{S}_p^t|)$. The time complexity for the server is $\mathcal{O}(2N_e + N_e \log(N_e) + \mathcal{Q}|\mathcal{S}_o^t| + (\mathcal{Q}+1)|\mathcal{S}_p^t|)$. Compared to the FedAvg framework [23], our framework increases the $\mathcal{O}(2N_e + N_e \log(N_e) + |\mathcal{S}_p^t|)$ time complexity.

Communication complexity: During a training round, the selected clients send their local models to the server. This communication process has a complexity of $\mathcal{O}(|\mathcal{S}_o^t| \sum + |\mathcal{S}_p^t| \sum)$, where \sum represents the model size. The server then aggregates the global model and sends it to the next selected clients, incurring a similar communication complexity of $\mathcal{O}(|\mathcal{S}_o^t| \sum + |\mathcal{S}_p^t| \sum)$.

VI. THEORETICAL ANALYSIS

A. Regret Bound for Training Interval

We examine the feasibility of biased client participation for both relevant and irrelevant clients. Unlike the probability form, we provide the regret bound of training interval $I(m)$ between two consecutive selections of the relevant client. If the length of training interval is small, the relevant client is more likely to participate into FL modeling. Firstly, we give the definition of the relevant and irrelevant clients.

Definition 1. (Relevant and irrelevant clients) A new client i_{ea} is considered as the relevant client from set $\mathcal{M}_{\tilde{p}}$ with $|\mathcal{M}_{\tilde{p}}| = \tilde{p}$, when the successful probability $u_{i_{ea}}$ is larger than the irrelevant client's probability $u_{i_{eb}}$ from set $\mathcal{M}_{N-\tilde{p}}$ with $|\mathcal{M}_{N-\tilde{p}}| = N - \tilde{p}$, i.e., $u_{i_{ea}} > \max_{i_{eb} \in \mathcal{M}_{N-\tilde{p}}} \{u_{i_{eb}}\}$.

Based on the above definition, the relevant client owns high successful probability to cause small path drift in the global model. The client participation group \mathcal{I}_e can be divided into two parts: $\mathcal{M}_{\tilde{p}}$ and $\mathcal{M}_{N-\tilde{p}}$, based on the true client participation size \tilde{p} . In addition, the definition of warm-up rounds [46], [47] is also present.

Definition 2. (Warm-up rounds condition) Over a total of T rounds, the irrelevant client i_{eb} has already been selected a sufficient number, i.e.,

$$L_{i_{eb}} = \frac{24 \ln T}{\Delta_{i_{ea}, i_{eb}}^2},$$

where $\Delta_{i_{ea}, i_{eb}} = u_{i_{ea}} - u_{i_{eb}}$ and $u_{i_{ea}} = \min\{u_{i_{ea}}\}_{i_{ea} \in \mathcal{M}_{\tilde{p}}}$.

Definition 2 provides a sufficient cumulative selection rounds that ensure more accurate estimation of the irrelevant client's $\mu_{i_{eb}}$. The client \hat{i}_{ea} is considered as the critical relevant client with the lowest successful probability in $\mathcal{M}_{\tilde{p}}$. If the irrelevant client's $\theta_{i_{eb}}^t$ exceeds the critical relevant client's $\theta_{\hat{i}_{ea}}^t$, the irrelevant client is selected at round t .

Let the set $C(t)$ contain irrelevant clients that satisfy the warm-up rounds condition. Next, the event $E_{i_{eb}}(t, \hat{i}_{ea})$ is defined as follows:

$$E_{i_{eb}}(t, \hat{i}_{ea}) : \left\{ \theta_{i_{eb}}^t \in \left[\mu_{i_{eb}} - \frac{\Delta_{i_{ea}, i_{eb}}}{2}, \mu_{i_{eb}} + \frac{\Delta_{i_{ea}, i_{eb}}}{2} \right] \mid i_{eb} \in C(t) \right\}, \quad (11)$$

where the event $E_{i_{eb}}(t, \hat{i}_{ea})$ indicates that the irrelevant client's sample is concentrated around its successful probability, establishing the connection between $\theta_{i_{eb}}^t$ and $\mu_{i_{eb}}$.

Lemma 1. Over a total of T rounds, the probability of event $E_{i_{eb}}(t, \hat{i}_{ea})$ satisfies

$$\Pr \left(E_{i_{eb}}(t, \hat{i}_{ea}) \mid s_{\hat{i}_{ea}}(m) \right) \geq 1 - \frac{4}{T^2}, \quad (12)$$

where $s_{\hat{i}_{ea}}(m)$ denotes the number of successful explorations in m -th selection of the critical relevant client \hat{i}_{ea} . The proof of this Lemma is provided in Appendix A.

Remark: From Lemma 1, the irrelevant client's $\theta_{i_{eb}}^t$ becomes tightly concentrated around its successful probability

$u_{i_{ea}}$ with high probability. Based on Lemma 1, the client participation search strategy is proposed. Additionally, this high-probability event will be utilized in the subsequent analysis.

Let $I(m)$ denote the training interval between the m -th and $m+1$ -th selections of the critical relevant client \hat{i}_{ea} . The expected regret bound for $I(m)$ is present.

Theorem 1. Based on the warm-up rounds condition, the expected regret of training interval $I(m)$ between two consecutive selections of the critical relevant client \hat{i}_{ea} is bounded as follows:

$$\begin{aligned} \mathbb{E} [\mathcal{R}(I(m))] &\leq 3\mathbb{E} [\mathbb{E} [\gamma_m + 1 \mid s_{\hat{i}_{ea}}(m)]] \\ &\cdot \mathbb{E} [\sum_{g \in \mathcal{M}_{N-\tilde{p}}} \Delta_{i_{ea}, g} \mathbb{E} [\min \{C, T\} \mid s_{\hat{i}_{ea}}(m)]] \\ &+ 2 \sum_{t \in I(m)} \mathbb{E} [\mathbb{I}(E_{i_{eb}}(t, \hat{i}_{ea}))], \end{aligned} \quad (13)$$

where $C = X \left(m, s_{\hat{i}_{ea}}(m), \mu_g + \frac{\Delta_{i_{ea}, g}}{2} \right)$ represents the number of trials until a sample from $\beta(s_{\hat{i}_{ea}}(m) + 1, m - s_{\hat{i}_{ea}}(m) + 1)$ exceeds $\mu_g + \frac{\Delta_{i_{ea}, g}}{2}$, $\mathbb{I}(\cdot)$ is the indicator function, and γ_m is the number of selection rounds of the irrelevant that can't satisfy warm-up rounds condition in training interval $I(m)$. The proof of this theorem is provided in Appendix B.

Remark: In the first term, γ_m is bounded by the total number of selection rounds for all irrelevant clients that cannot satisfy warm-up rounds condition, i.e., $O(\sum_{i_{eb} \in \mathcal{M}_{N-\tilde{p}}} L_{i_{ea}, i_{eb}})$. From [46], the $\mathbb{E}[\mathbb{E} [\min \{C, T\} \mid s_{\hat{i}_{ea}}(m)]]$ is bounded by $O(\frac{1}{\Delta_{i_{ea}, i_{eb}}})$, and it is bounded by $O(\sum_{i_{eb} \in \mathcal{M}_{N-\tilde{p}}} L_{i_{ea}, i_{eb}})$ as well. This gives a bound of $O((\sum_{i_{eb} \in \mathcal{M}_{N-\tilde{p}}} \frac{\ln T}{\Delta_{i_{ea}, i_{eb}}^2})^2)$ on above. In the second term, $\mathbb{I}(E_{i_{eb}}(t, \hat{i}_{ea}))$ is bounded by the low probability of event $E_{i_{eb}}(t, \hat{i}_{ea})$. Theorem 1 proves a weaker bound of $O((\ln T)^2)$ on the expected regret. Given the adequate client selection rounds (i.e., $\sum_{i_{eb} \in \mathcal{M}_{N-\tilde{p}}} L_{i_{ea}, i_{eb}}$) for the client \hat{i}_{ea} , the sample will be sufficiently concentrated around its successful probability. This leads to a very low probability of selecting any irrelevant clients that satisfy the warm-up rounds condition.

B. Convergence Analysis

In this subsection, we provide the convergence analysis of the Fed-TS framework. Some necessary assumptions will be introduced.

Assumption 1. Each f_i is L_p -smooth. For \mathbf{w}, \mathbf{w}' , we have that

$$\|\nabla f_i(\mathbf{w}) - \nabla f_i(\mathbf{w}')\|^2 \leq L_p \|\mathbf{w} - \mathbf{w}'\|^2, \quad (14)$$

where $\nabla f_i(\mathbf{w})$ denotes the client's stochastic gradient.

Assumption 2. The variance of local gradients $\nabla f_i(\mathbf{w})$ to global gradients $\nabla F(\mathbf{w})$ is bounded, i.e.,

$$\|\nabla f_i(\mathbf{w}) - \nabla F(\mathbf{w})\|^2 \leq \sigma_{F,i}^2, \quad \forall i, \mathbf{w}. \quad (15)$$

From previous works [48], [49], L_p -smoothness assumption is necessary for the convergence analysis in FL. Unlike

using the assumption of bounded gradients, we consider the bounded diversity between the client gradients $\nabla f_i(\mathbf{w})$ and global gradients $\nabla F(\mathbf{w})$ [50], [51]. Furthermore, work [51] provides the specific formulation of $\sigma_{F,i}^2$ (i.e., $\sigma_{F,i}^2 = \kappa - \rho e^{\beta(H(\mathcal{D}_i) - H(\mathcal{D}_F))}$, where \mathcal{D}_i is the data distribution of i -th client, \mathcal{D}_F denotes uniform distribution, $H(\cdot)$ is Shannon's entropy of a stochastic vector, and $\beta > 0, \kappa > \rho > 0$). In our paper, the new participating irrelevant client has low-quality or incorrect data, which affects $H(\mathcal{D}_i)$.

Lemma 2. (*Participating client diversity bound*) *Given the hyper-parameter ε and adaptive threshold $\alpha^{(t)}$ from the proposed framework, the participating client diversity $\|\mathbf{w}_{oe}^{(t)} - \mathbf{w}_o^{(t)}\|^2$ can be bounded as follows:*

$$\|\mathbf{w}_{oe}^{(t)} - \mathbf{w}_o^{(t)}\|^2 \leq \frac{(|\mathcal{S}_o^t| + \varepsilon)^2 |\mathcal{S}_p^t|^2}{(|\mathcal{S}_o^t| + |\mathcal{S}_p^t|)^2 \varepsilon^2} \alpha^{(t)}, \quad (16)$$

where the proof can be found in Appendix C.

Remark: In fact, $\|\mathbf{w}_{oe}^{(t)} - \mathbf{w}_o^{(t)}\|^2$ quantifies the diversity between $\mathbf{w}_{oe}^{(t)}$ (the global model with client participation) and $\mathbf{w}_o^{(t)}$ (the global model without client participation). For fixed ε , $|\mathcal{S}_o^t|$ and $|\mathcal{S}_p^t|$, Lemma 2 indicates that the upper bound of participating client diversity is limited by the value of $\alpha^{(t)}$. Lemma 2 is used in the proof of the convergence analysis.

Theorem 2. (*Convergence bound*) *If Assumptions 1 and 2 hold. Suppose that the insertion time is t_0 . There exists an $\eta \leq \frac{\tilde{\eta}}{R}$, where $\tilde{\eta} \leq \frac{1}{(6 + \frac{60 \ln(1+1/R)}{R})L_p} \leq \frac{1}{2L_p}$, such that*

$$\begin{aligned} \frac{1}{T} \sum_{t=1}^T \mathbb{E} \left\| \nabla F \left(\mathbf{w}_{oe}^{(t)} \right) \right\|^2 &\leq \mathcal{O} \left(\frac{\mathbb{E} \left\| \mathbf{w}_o^{(t_0)} - \mathbf{w}_o^* \right\|^2}{\tilde{\eta} T} \right) + \mathcal{O} \left(\frac{\Delta_{\alpha_{t_0}}}{\tilde{\eta} T} \right) \\ &\quad + \mathcal{O} \left(CL_p \max_{i \in \mathcal{I}} \{ \sigma_{F,i}^2 \} \tilde{\eta} \right), \end{aligned} \quad (17)$$

where $\Delta_{\alpha_{t_0}} = W (\alpha^{(t_0)} + \alpha^{(T^*)})$ with $W = \frac{3L(|\mathcal{S}_o^t| + \varepsilon)^2 |\mathcal{S}_p^t|^2}{2(|\mathcal{S}_o^t| + |\mathcal{S}_p^t|)^2 \varepsilon^2}$, T^* represents the specific training round corresponding to the unique solution \mathbf{w}_{oe}^* ; $C = \frac{3L(N/S-1)}{2(N-1)} + \frac{15L \ln(1+1/R)}{R}$, $N = N_o + N_e$, and $S = |\mathcal{S}_o^t| + |\mathcal{S}_p^t|$; $\max_{i \in \mathcal{I}} \{ \sigma_{F,i}^2 \}$ represents the largest client's variance with $\mathcal{I} = \mathcal{I}_o \cup \mathcal{I}_e$; $\mathcal{O}(\cdot)$ contains the constant factors; In addition, R , η and $\tilde{\eta}$ are defined in Appendix D. The proof of this theorem is also found in Appendix D.

Remark: The first term, specifically $\mathcal{O}(\mathbb{E} \|\mathbf{w}_o^{(t_0)} - \mathbf{w}_o^*\|^2)$, represents the FL modeling process in a scenario with no participating clients. Therefore, we have $\mathcal{O}(\mathbb{E} \|\mathbf{w}_o^{(t_0)} - \mathbf{w}_o^*\|^2) \propto \mathcal{O}(\mathbb{E} \|\nabla F_o(\mathbf{w}_o^{(t_0)})\|^2)$, which aligns with the results from previous work [48]. For the second term, we focus on the value of $\alpha^{(T^*)}$ in $\mathcal{O}(\Delta_{\alpha_{t_0}})$. As discussed in Subsection V-C, we have $\alpha^{(t)} \propto \mathcal{S}_p^t$, meaning that the value of $\alpha^{(t)}$ is determined by the selected client set \mathcal{S}_p^t . According to Theorem 1, under the warm-up rounds condition, the probability of selecting irrelevant clients is low. Assuming that after the t_w -th round, each irrelevant client i_{eb} from $\mathcal{M}_{N-\tilde{p}}$ has completed its corresponding warm-up rounds $L_{i_{eb}}$. Consequently, after the t_w -th round, the selected client set \mathcal{S}_p^t includes relevant clients with small path drift, leading to a small value of $\alpha^{(t)}$.

TABLE I
THE INDEX OF RELEVANT CLIENTS ACROSS DIFFERENT CONSTRUCTED SCENARIOS

Scenarios	Data	The index of relevant clients
Label-flipping attack	CIFAR-10-L	20,21,22,23,24,25,26,27,28,29
	Fashion-MNIST-L	18,19,20,21,22,23,24,25,26
	AG-news-L	15,16,17,18,19
Data heterogeneity	CIFAR-10-Q	10,11,12,13,14
	Fashion-MNIST-Q	16,17,18,19,20,21,22,23
	AG-news-Q	15,16,17,18,19
Model-poisoning attack	CIFAR-10-M	16,17,18,19,20,21,22,23
	Fashion-MNIST-M	10,11,12,13,14
	AG-news-M	16,17,18,19,20,21,22,23

Noting that T^* is larger than t_w , $\alpha^{(T^*)}$ remains a small value. Consequently, our framework can provide the lower bound for $\mathcal{O}(\Delta_{\alpha_{t_0}})$. Finally, the proposed framework achieves a convergence speedup of $\mathcal{O}(\frac{1}{T})$ for the global model.

VII. EXPERIMENTS AND RESULTS

A. Datasets and Related Models

We examine our proposed framework under three public datasets. The details of the datasets and the related models used are summarized below:

- CIFAR-10 dataset consists of 60000 32×32 color images in 10 categories, including 50000 samples for training and 10000 samples for testing. The convolutional neural networks (CNN) model consists of two 5×5 convolution layers with 6 channels and 16 channels, respectively. Each layer is connected with a 2×2 maximum pooling layer. Two full connection layers are considered, consisting of the ReLu activation function and softmax output layer.
- Fashion-MNIST dataset consists of 70000 28×28 clothing images, with 60000 training images and 10000 testing images for 10 categories. We use the convolutional neural networks (CNN) model. This model contains two 5×5 convolution layers with 16 channels and 32 channels. Each convolutional layer is followed by BN layers, Relu activation, and maximum pooling. Finally, a fully connected layer with a linear activation function is used.
- AG-News dataset is a standard benchmark dataset for text classification, comprising 127600 news articles from English news websites with four topic categories. In this paper, the transformer model is used to testify the proposed framework. Moreover, the basic configuration of the transformer model can be found in [52].

B. Implementation Details

During the experiments, three types of scenarios are constructed to simulate the dynamic participating client scenario.

Label-flipping attack scenario: In this scenario, the label-flipping attack strategy is utilized to simulate malicious client attacks. Label-flipping attack strategy [53] involves changing the class labels of the client. For the CIFAR-10 dataset, we designate 10 original clients

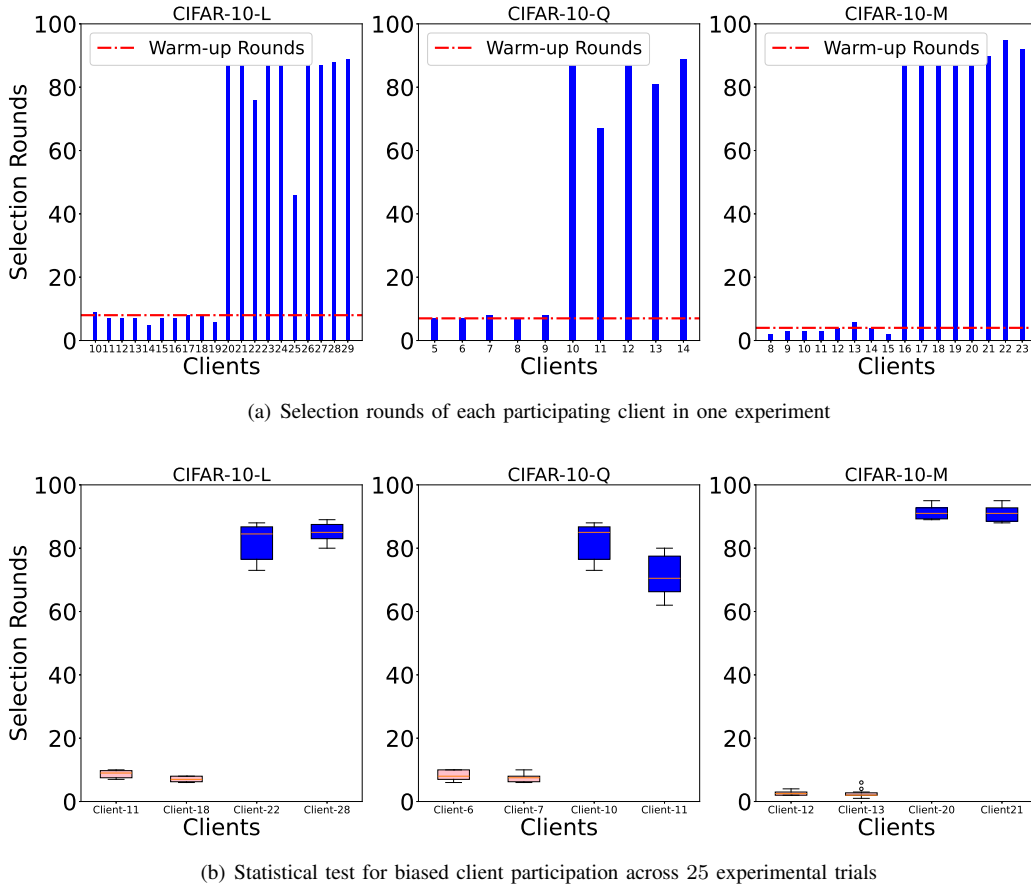


Fig. 5. The experimental results in the CIFAR-10 dataset with $P = 0.5$.

with labels indexed by $\{0, 2, 4, 6, 8\}$. At the 10-th round, both the 10 clients with labels indexed by $\{0, 2, 4, 6, 8\}$ and an additional 10 clients with labels indexed by $\{1, 3, 5, 7, 9\}$ will be included in the FL system. For the Fashion-MNIST dataset, at the 10-th round, 9 clients with labels indexed by $\{0, 2, 4, 6, 8\}$ and 9 clients with labels indexed by $\{1, 3, 5, 7, 9\}$ will be added to the original system, which already includes 9 clients with labels indexed by $\{0, 2, 4, 6, 8\}$. For the AG-news dataset, at the 10-th round, 5 clients with labels indexed by $\{0, 2, 4, 6, 8\}$ and 5 clients with labels indexed by $\{1, 3, 5, 7, 9\}$ come into the original system, which already includes 5 clients with labels indexed by $\{0, 2, 4, 6, 8\}$.

Model-poisoning attack scenario: In the model-poisoning attack scenario, malicious clients provide incorrect gradient information to affect the performance of the global model. For this scenario, new participating malicious clients upload random-zero-mean gaussian gradient [55] to the server. For the CIFAR-10 dataset, we set 8 benign clients as original client group. At the 10-th round, 8 malicious clients and 8 benign clients come into original client group. For the Fashion-MNIST dataset, at the 10-th round, 5 malicious clients and 5 benign clients will be added to the original system, which already includes 10 benign clients. For the AG-news dataset, at the 10-th round, 8 malicious clients and 8

benign clients will be added to the original system, which already includes 8 benign clients.

Data heterogeneity scenario: The quantity skew strategy [54] is considered to construct the data heterogeneity scenario, in which clients share the same class labels but different sample distributions. For the CIFAR-10 dataset, we establish 10 clients with similar data sizes for each label. 5 of these clients are selected as original client group, while the remaining 5 serve as participation client group. At the 10-th round, an additional 5 clients, each with varying data sizes for each label, are incorporated into original FL modeling process. Similarly, for the Fashion-MNIST dataset, we choose 8 clients with similar data sizes for each label to original client group. At the 10-th round, 8 clients with similar data sizes and 8 clients with varying data sizes for each label come into original client group. For the AG-news dataset, we set up 5 clients, each with a similar data size for each label. At the 10-th round, an additional 5 clients with varying data sizes and 5 clients with similar data sizes, will participate into original client group.

Table I summarizes the index of relevant clients across constructed scenarios, which will be used to evaluate the biased client participation performance of the proposed framework. In Subsection VII-G, we will consider the large-scale devices scenario. In addition, the public

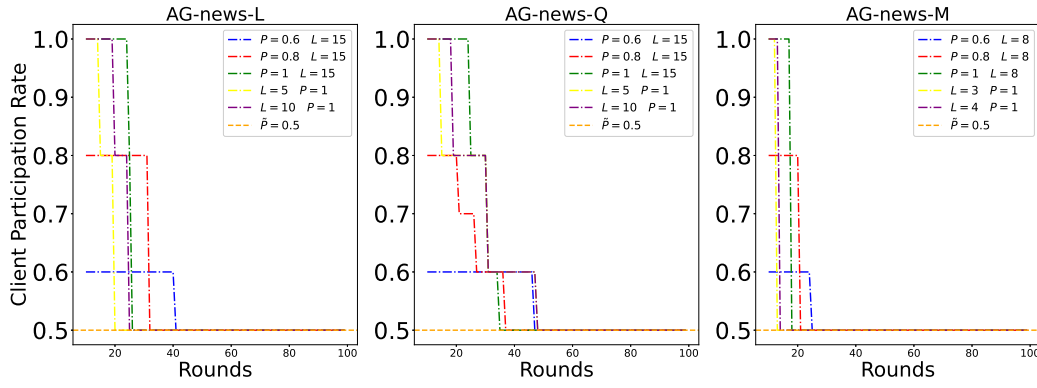


Fig. 6. Process of client participation size search strategy in the AG-news dataset. \hat{P} is the true client participation rate. P and L are the original participation size and the threshold, respectively.

hyper-parameters of our framework are summarized in Appendix E.

C. Discussion of Client Participation Size

The discussion of client participation rate is to verify the two cases in the client participation phase. In this experiments, we adopt client participation rate P to control the client participation size p . For instance, when $P = 0.5$, it means that half of the clients will be selected at each round. We note that the true client participation rate \hat{P} is 0.5. According the two cases, the relationships between set client participation rate P and true client participation rate \hat{P} are summarized as: $P = \hat{P} = 0.5$ (Case 1) and $P > 0.5$ (Case 2).

Case 1: Fig. 5 presents the experimental results in the CIFAR-10 dataset. Specifically, Fig. 5 (a) presents the selection rounds of each new participating client under three scenarios. We can observe that each relevant client achieves a higher number of selection rounds, facilitating a clearer distinction between both relevant and irrelevant clients. According to Theorem 1, when P equals \hat{P} , the presence of warm-up rounds of irrelevant clients is also noted (indicated by red line). It confirms that as the irrelevant client nears its warm-up rounds, the likelihood of being selected will decrease accordingly. Meanwhile, Fig. 5 (b) shows the statistical test for biased client participation. Over 25 experimental trials, our framework also guarantees a significant difference in selection rounds between irrelevant clients and relevant clients.

Case 2: In this case, the true client participation rate is unknown, which better reflects the real-world scenario. Fig. 6 shows the process of client participation size search strategy in the Fashion-MNIST dataset. When $P = 1$ and $L = 4$, all new participating clients come into training process until each client's selection rounds exceeds L , at which point the search strategy will be implemented. In the label-flipping attack scenario, our framework achieves the shortest search rounds when $P = 1$ and $L = 5$. Similarly, the proposed algorithm achieves the shortest search rounds in the model-poisoning attack and data

heterogeneity scenarios when $P = 1$ and $L = 3$, as well as when $P = 1$ and $L = 15$. It can be observed that a larger value of P can quickly search the true participation rate. According to Lemma 1, L should be equal to the irrelevant client's warm rounds. In practice, considering the potential impact of malicious clients, it is advisable to set lower values for L in our framework, allowing for a quicker achievement of biased participation for these clients. In the data heterogeneity scenario, we recommend that using low P to avoid the decline in global model's accuracy during the initial training phase. In addition, Fig. 7 shows the experimental results in the AG-news dataset with $P > 0.5$. It can find that relevant clients have a significant higher number of selection rounds, while irrelevant clients have fewer selections. Across 15 experimental trials, the proposed framework consistently achieves a greater number of selection rounds for relevant clients. For instance, in the model-poisoning attack scenario, the average number of selection rounds among relevant clients is approximately 88.

D. Impact of the Aggregation Weight

Firstly, we give the practical guidance on the aggregation weight ε . This hyper-parameter determines the contribution of one participating client to the global model. Fig. 8 presents the number of successful or failed explorations of the participating client with $\varepsilon = 1$ and $\varepsilon = 5$ (equal weights for both the original client group and the new participating client). In the data heterogeneity scenario, the aggregation weight for a participating client is $\frac{1}{6}$ when $\varepsilon = 1$, and it increases to $\frac{1}{2}$ when $\varepsilon = 5$. In Fig. 8 (a), from $\varepsilon = 1$ to $\varepsilon = 5$, the number of successful explorations for the relevant client (observed by the 14-th client) increases from 41 to 76. In Fig. 8 (b), for the irrelevant client (observed by the 9-th client), the number of selection rounds decreases as ε increases from 1 to 5. Especially, when $\varepsilon = 5$, the proportion of failed explorations is high, leading to a low participation probability of the irrelevant client. In terms of practical guidance, we introduce $\|\mathbf{w}_{oi_e} - \mathbf{w}_o\|^2$ to measure the path drift of the client i_{ea} to the original global model. We can view the original client group as

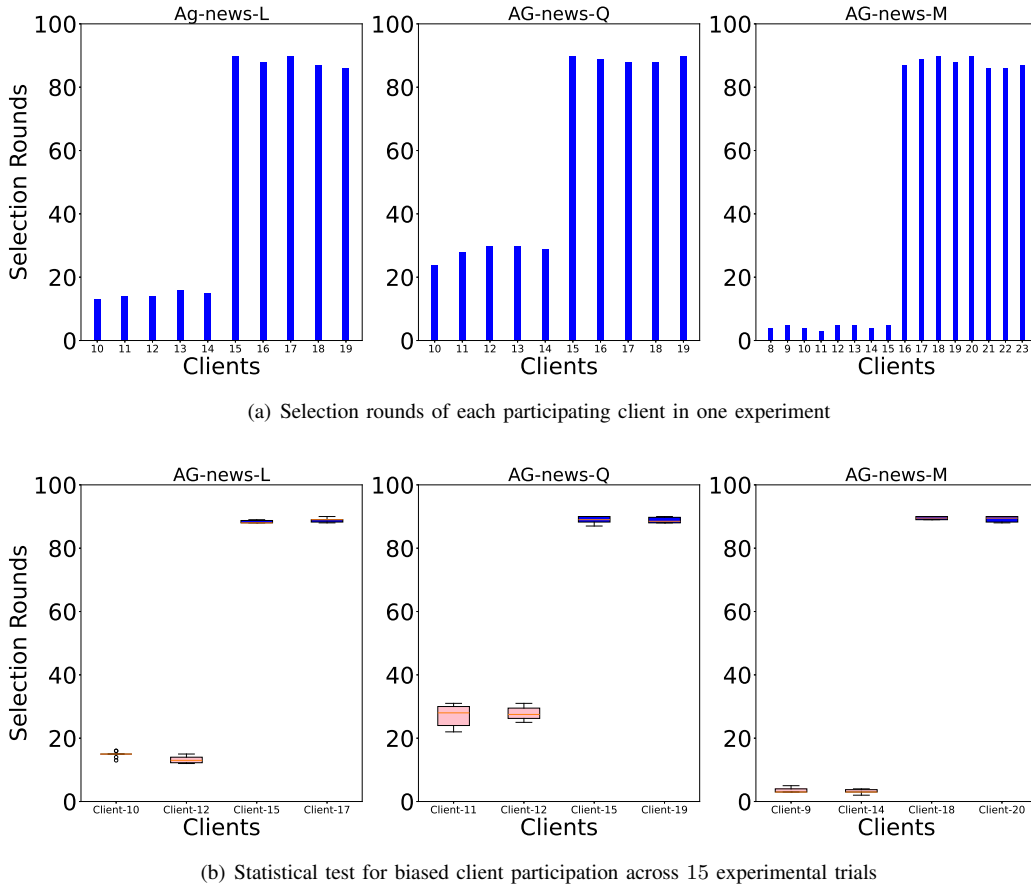


Fig. 7. The experimental results in the AG-news dataset with $P > 0.5$; AG-news-L: $P = 1, L = 5$; AG-news-Q: $P = 0.8, L = 15$; AG-news-M: $P = 1, L = 3$.

a system. Equal weights for both the original client group and the new participating client can effectively reflect the impact of the new participating clients on the original global model. In our framework, we recommend setting ε equal to the sampling size of original client group, $|\mathcal{S}_o^t|$, to ensure equal weights for both systems.

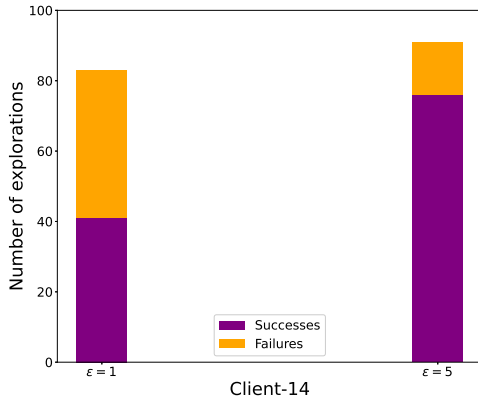
E. Comparison with Other Schemes

In this subsection, we compare the predictive performance of the proposed framework with the following schemes:

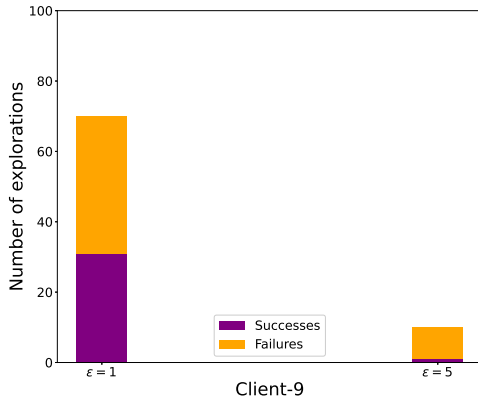
- Random [24]: A widely client participation scheme in FL involves randomly selecting a certain proportion of clients at each round.
- Pow-d [25]: A client participation scheme that selects clients with high loss values at each round.
- PNS [26]: A client participation scheme to find valuable clients based on the output of optimal aggregation.
- CHR [23]: A robust scheme to ensure the stability and accuracy of the model through employing cosine similarity to measure global and local gradients.
- UCB [32]: A client participation scheme to select the top clients with the higher upper confidence bound.
- MARL [56]: An efficient scheme to perform client participation based on reinforcement learning.

- Oort [57]: An efficient strategy to improve the robustness of model performance with guided participant selection.

Fig. 9 shows the test accuracy of different schemes. In the context of malicious attack scenario, new irrelevant clients may provide modified data or incorrect gradient information, potentially harming the global model. Specifically, in the model-poisoning attack scenario, the accuracy curves of the Random, Pow-d, CHR, PNS, UCB, and Oort schemes exhibit a significant decline after the 10th round (the insertion time). These schemes rely on prior information (such as loss functions [25], statistical utility [32], [56], [57], gradient information [26], and path drift [23]) to facilitate biased client participation. However, they fail to effectively exclude irrelevant clients among potential new participants. The MARL scheme, based on RL, aims to constrain the upward update of testing accuracy, thereby ensuring the robustness of the global model. However, this approach requires searching for combinations of new participating clients, resulting in high time complexity. In contrast, our framework enables biased participation from both irrelevant and relevant clients, leading to the development of a robust global model. In the AG-News dataset, the test curve initially shows a downward trend, which can be attributed to Algorithm 3 searching for the true client participation size during the early training rounds. Furthermore, in the scenarios of data heterogeneity, clients



(a) The number of successful or failed explorations of the relevant client.



(b) The number of successful or failed explorations of the irrelevant client.

Fig. 8. The number of successful or failed explorations of the participating client in the CIFAR-10 dataset with $\epsilon = 1$ and 5.

with low-quality data also degrade the model's performance. In such cases, our framework still achieves higher test accuracy.

F. Comparison with Other FL Frameworks

In this subsection, the Fed-TS framework is compared against other FL frameworks which can alleviate data heterogeneity. We study the test accuracy by the global model of FedProx [13], FedBN [14], SCAFFOLD [16], FedGen [17], FedDyn [15], MOON [18], FedAdam [34], FedYogi [34], GOFL [35] and FedREM [19] frameworks. Both our framework and the FedREM framework are designed for dynamic client participating scenarios, while the other frameworks focus on static scenarios. To ensure a fair comparison, we upload the global model from the 10-th round to the local clients for the static FL frameworks, leading to a total of 90 rounds. Due to the model limitations of the FedREM framework, our comparisons are restricted to the Fashion-MNIST dataset. In addition, we construct the feature skew scenario based on the Dirichlet distribution [58], i.e. $q \sim \text{Dir}(d)$, where q is a prior class distribution over labels and d is a parameter controlling the distribution among clients. In the Fashion-MNIST dataset,

TABLE II
BEST TEST ACCURACY COMPARISON OF DIFFERENT FRAMEWORKS UNDER TWO SCENARIOS IN THE FASHION-MNIST DATASET

Scenarios	Methods	Best Test Accuracy
Extreme data heterogeneity	FedProx	73.45%
	FedBN	72.45%
	SCAFFOLD	70.20%
	FedGen	67.55%
	FedDyn	75.31%
	MOON	68.39%
	GOFL	69.33%
	FedAdam	74.29%
	FedYogi	74.71%
	FedREM	76.73%
Model-poisoning attack	Our	79.56%
	FedProx	48.35%
	FedBN	66.74%
	SCAFFOLD	73.61%
	FedGen	56.50 %
	FedDyn	55.77%
	MOON	58.19%
	GOFL	60.01%
	FedAdam	62.22%
	FedYogi	64.33%
	FedREM	67.60%
	Our	85.37%

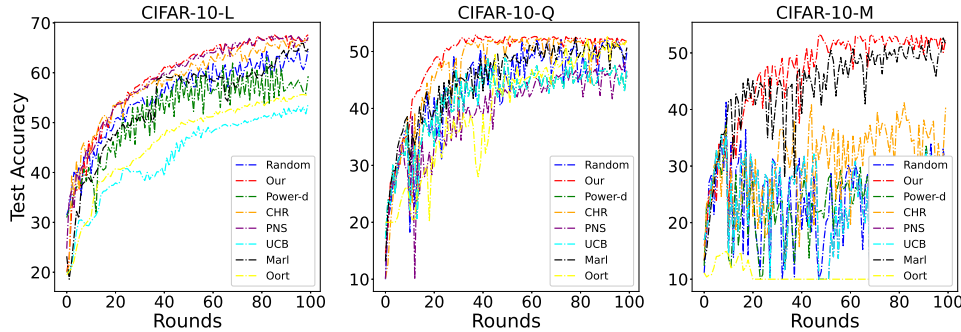
the original client group is assigned a value of $q = 5$, while all irrelevant clients from the participation group are assigned $q = 0.5$.

Table II shows the experimental results. From the table, our framework outperforms FedREM framework by 2.83% in the extreme data heterogeneity scenario. The reason is that the FedREM framework helps additional clients adapt to the global model to address data heterogeneity issues. However, in the face of adversarial attack scenarios (i.e., when malicious clients provide forged models), the FedREM framework fails, achieving a test accuracy of 67.60%, compared to our framework, which achieves 85.37%. Our framework tackles the challenge of model-poisoning attack by employing a biased client participation approach from the clients' perspective.

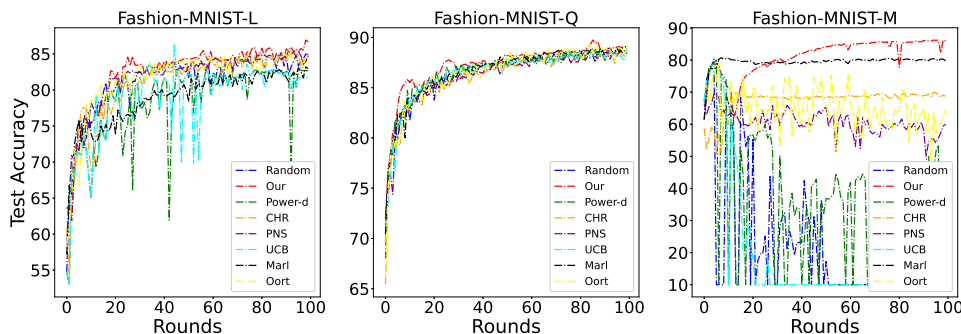
G. Scalability of the Proposed Framework

Firstly, we test our framework in the system heterogeneous setting. The system heterogeneous setting is summarized as follows:

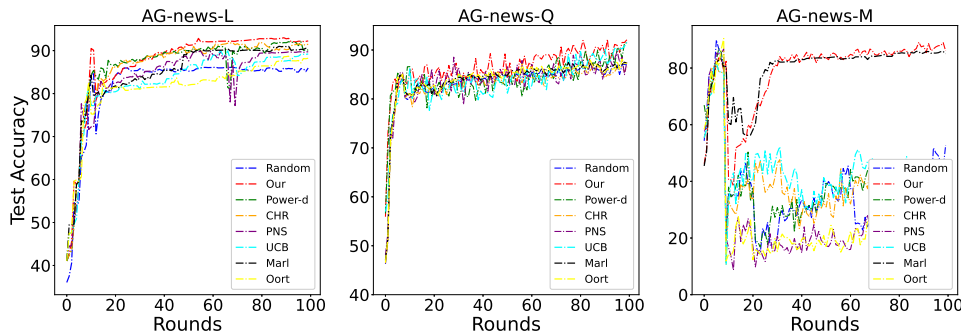
- Large-scale devices: A total of 250 devices is simulated. Of these, 50 devices constitute the initial client group \mathcal{I}_o , while the remaining 100 devices—comprising 100 relevant devices and 100 irrelevant devices—are incorporated into the initial client group. We consider the model-poisoning attack scenario.
- Multiple insertion times: We set the multiple insertion times set $\{t_0, t_1, t_2, t_3\}$ and the corresponding new client group set $\{\mathcal{I}_{e0}, \mathcal{I}_{e1}, \mathcal{I}_{e2}, \mathcal{I}_{e3}\}$. At round t_0 , new client group \mathcal{I}_{e0} (including 25 relevant clients and 25 irrelevant clients) participate into FL modeling process.
- The dropout devices: Following by [35], we allow each device i to perform different local epochs, i.e., $\{2, 3, 4, 5\}$. Meanwhile, the dropout client rate $P_d = 0.2$ is set to simulate the indirect exit of clients due to resource constraints.



(a) CIFAR-10 dataset with $P = 0.5$



(b) Fashion-MNIST dataset with $P > 0.5$; Fashion-MNIST-L: $P = 1, L = 8$; Fashion-MNIST-Q: $P = 0.8, L = 14$; Fashion-MNIST-M: $P = 1, L = 4$



(c) AG-news dataset with $P > 0.5$; AG-news-L: $P = 1, L = 5$; AG-news-Q: $P = 0.8, L = 15$; AG-news-M: $P = 1, L = 3$.

Fig. 9. Test accuracy comparison of different schemes.

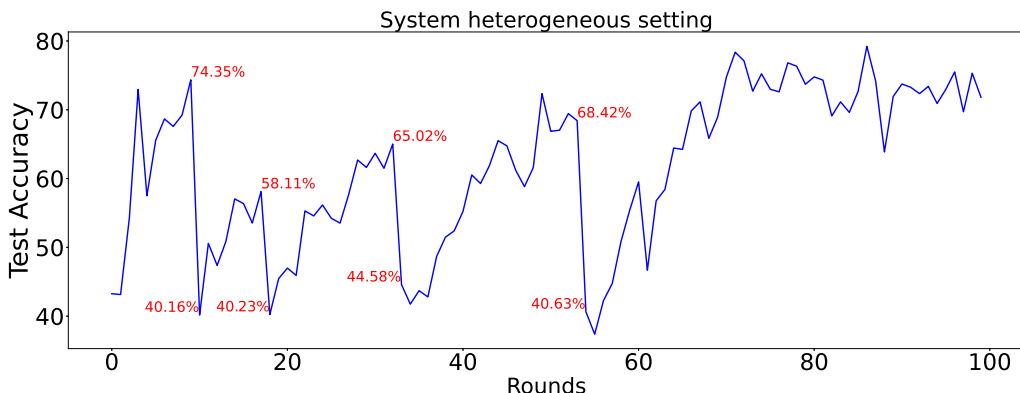
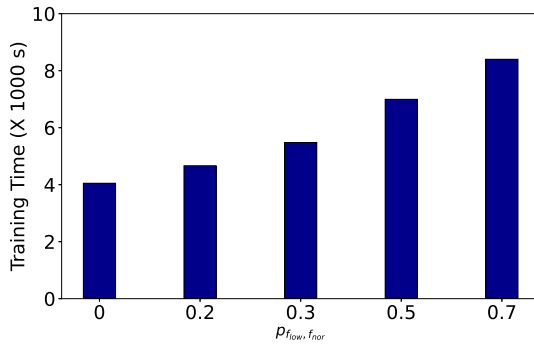


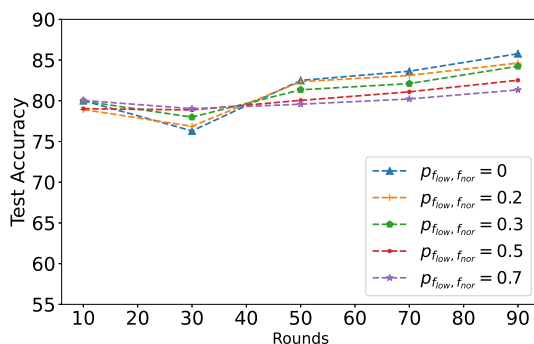
Fig. 10. The test accuracy of the Fed-TS framework in the AG-news dataset. The insertion times set is $\{11, 19, 35, 56\}$. For each client participation group, the Fed-TS framework combines with the client participation size search strategy with $P = 1$ and $L = 3$.

From Fig. 10, the participation of new client groups can lead to a decline in the test accuracy of the global model. Specifically, at round 16, the accuracy drops from 74.35% to 40.16%. At round 19, it decreases from 58.11% to 40.23%. At round 35, the accuracy falls from 65.02% to 44.58%, and at round 56, it declines from 68.42% to 40.63%. After round 56, the accuracy begins to increase and remains stable. Essentially, our framework utilizes a posterior Beta distribution to store the information of successful and failed explorations for each participating device, drawn from the corresponding Beta distribution determine whether these specific clients participate into FL modeling.

Next, we investigate the performance of our framework in resource-constrained scenarios. All experiments achieve resource-constrained scenarios by adjusting the CPU frequency [59], [60]. Two CPU frequency ranges are set: $f_{nor} = [1GHz, 3GHz]$ (the frequency range for smartphones [60]) and $f_{low} = [0.1GHz, 1GHz]$. In this experiment, a proportion of $p_{f_{low}, f_{nor}}$ of the new participating devices will operate within the f_{low} frequency range.



(a) The training times achieved with 85% accuracy under various $p_{f_{low}, f_{nor}}$.



(b) The test accuracy under various $p_{f_{low}, f_{nor}}$.

Fig. 11. Experimental results with various $p_{f_{low}, f_{nor}}$ in the Fashion-MNIST dataset.

Fig. 11 (a) shows the training time achieved with 85% accuracy. We also consider the model-poisoning attack scenario. As $p_{f_{low}, f_{nor}}$ increases, the training time rises as well. This is attributed to the new client operating at a CPU frequency within the f_{low} range, which leads to extended training time for modeling tasks. Additionally, within a fixed time slot and under resource-constrained conditions, the occurrence of

stragglers is also unavoidable. Fig. 11 (b) presents the test accuracy under various $p_{f_{low}, f_{nor}}$. When $p_{f_{low}, f_{nor}} = 0$, the proposed framework experiences a decline in test accuracy during the initial rounds. In fact, resource-constrained devices can limit the participation of irrelevant clients, which in turn enhances the model's robustness. However, compared to the non-resource-constrained setting, the framework exhibits lower test accuracy as training progresses.

VIII. CONCLUSION

In this paper, we consider a specific FL scenario where new clients dynamically participate into modeling process. In particular, new participating clients with irrelevant data decrease the accuracy of the global model. To address this challenge, we introduce the TS policy, a reinforcement learning (RL) approach, into our framework to achieve biased client participation for both relevant and irrelevant clients. Especially during the client participation phase, the multiple-play Thompson sampling (MP-TS) algorithm is employed. During the distribution updating phase, the successful probability of causing “small path drift” in the global model is utilized to update the posterior Beta distribution of the selected clients. Meanwhile, an adaptive threshold, derived from the K -means algorithm, is implemented to assess “small path drift” in the global model. We provide a regret bound for the training interval between two selections of the relevant client. The convergence analysis is also provided. For all experiments, we evaluate the performance of the framework in data heterogeneity and malicious attack scenarios. We examine the impact of hyperparameters on the performance of biased participation for both relevant and irrelevant clients. Additionally, we compare our framework with other existing schemes, and the results demonstrate that our proposed framework achieves a robust global model with high accuracy. Finally, the scalability of the proposed framework is considered.

From a security perspective, our framework may face threats such as inference attacks and backdoor attacks. In future work, we plan to implement differential privacy techniques to protect model information.

APPENDIX

A. Proof of Lemma 1

Review that event $E(t, \hat{i}_{ea})$ is formulated in (11). Firstly, we bound $\Pr(E(t, \hat{i}_{ea}) | s_{\hat{i}_{ea}}(m))$ as follows:

$$\begin{aligned} \Pr(E_{i_{eb}}(t, \hat{i}_{ea}) | s_{\hat{i}_{ea}}(m)) &\leq \underbrace{\Pr(E_{i_{eb}}^+(t, \hat{i}_{ea}) | s_{\hat{i}_{ea}}(m))}_{A_1} \\ &+ \underbrace{\Pr(E_{i_{eb}}^-(t, \hat{i}_{ea}) | s_{\hat{i}_{ea}}(m))}_{A_2}. \end{aligned} \quad (18)$$

Here, $E_{i_{eb}}^+(t, \hat{i}_{ea})$ denotes the event defined as

$$\left\{ \theta_{i_{eb}}^t \geq \mu_{i_{eb}} + \frac{\Delta_{\hat{i}_{ea}, i_{eb}}}{2} \text{ or } i_{eb} \notin C(t) \right\},$$

while $E_{i_{eb}}^-(t, \hat{i}_{ea})$ represents the event defined as

$$\left\{ \theta_{i_{eb}}^t \leq \mu_{i_{eb}} + \frac{\Delta_{\hat{i}_{ea}, i_{eb}}}{2} \text{ or } i_{eb} \notin C(t) \right\}.$$

For A_1 , we note that

$$\begin{aligned} & \Pr\left(\overline{E_{i_{eb}}^+(t, \hat{i}_{ea})} \mid s_{\hat{i}_{ea}}(m)\right) \\ &= \Pr\left(\theta_{i_{eb}}(t) > \mu_{i_{eb}} + \frac{\Delta_{\hat{i}_{ea}, i_{eb}}}{2}, k_{i_{eb}}(t) \geq L_{i_{eb}} \mid s_{\hat{i}_{ea}}(m)\right), \end{aligned} \quad (19)$$

where $k_{i_{eb}}(t)$ is the number of selection rounds of client i_{eb} until round $t - 1$.

Let us define the event $A_{i_{eb}}(t)$ as follows:

$$A_{i_{eb}}(t) : \frac{S_{i_{eb}}(t)}{k_{i_{eb}}(t)} \leq \mu_{i_{eb}} + \frac{\Delta_{\hat{i}_{ea}, i_{eb}}}{4}, \quad (20)$$

where $S_{i_{eb}}(t)$ is the number of successful explorations of client i_{eb} until time $t - 1$. Consequently, (19) is bounded as follows:

$$\begin{aligned} & \Pr\left(\overline{E_{i_{eb}}^+(t, \hat{i}_{ea})} \mid s_{\hat{i}_{ea}}(m)\right) \\ &\leq \underbrace{\Pr\left(A_{i_{eb}}(t), k_{i_{eb}}(t) \geq L_{i_{eb}} \mid s_{\hat{i}_{ea}}(m)\right)}_{B_1} + \\ &\quad \underbrace{\Pr\left(\theta_{i_{eb}}(t) > \mu_{i_{eb}} + \frac{\Delta_{p,i}}{2}, k_{i_{eb}}(t) \geq L_{i_{eb}}, A_{i_{eb}}(t) \mid s_{\hat{i}_{ea}}(m)\right)}_{B_2}. \end{aligned} \quad (21)$$

Next, we define $Z_{i,m}$ and $\bar{Z}_{i,M}$. Here, $Z_{i,d}$ represents the Bernoulli variable (successful or failed explorations) of the m -th selection of client i , and,

$$\bar{Z}_{i,D} = \frac{1}{D} \sum_{d=1}^D Z_{i,d}. \quad (22)$$

Based on the above definitions, the B_1 is bounded as follows:

$$\begin{aligned} B_1 &= \sum_{\ell=L_{i_{eb}}}^T \Pr(\bar{Z}_{i_{eb},\ell} > \mu_{i_{eb}} + \frac{\Delta_{\hat{i}_{ea}, i_{eb}}}{4}, k_{i_{eb}}(t) = \ell \\ &\quad \mid Z_{\hat{i}_{ea},1}, \dots, Z_{\hat{i}_{ea},m}) \\ &\leq \sum_{\ell=L_{i_{eb}}}^T \Pr\left(\bar{Z}_{i_{eb},\ell} > \mu_{i_{eb}} + \frac{\Delta_{\hat{i}_{ea}, i_{eb}}}{4} \mid Z_{\hat{i}_{ea},1}, \dots, Z_{\hat{i}_{ea},m}\right) \\ &= \sum_{\ell=L_{i_{eb}}}^T \Pr\left(\bar{Z}_{i,\ell} > \mu_{i_{eb}} + \frac{\Delta_{\hat{i}_{ea}, i_{eb}}}{4}\right) \\ &\leq \sum_{\ell=L_{i_{eb}}}^T e^{-2\ell\Delta_{\hat{i}_{ea}, i_{eb}}^2/16} \leq \frac{1}{T^2}. \end{aligned} \quad (23)$$

The first inequality holds because $\bar{Z}_{i_{eb},\ell}$ is independent of $Z_{\hat{i}_{ea},d}$ for all $d = 1, \dots, m$. The second inequality is due to Chernoff-Hoeffding bounds [37].

For B_2 , the upper bound is provided as follows:

$$\begin{aligned} & B_2 \\ &= \sum_{\ell=L_{i_{eb}}}^T \Pr\left(\theta_{i_{eb}}^t \geq \mu_{i_{eb}} + \frac{\Delta_{\hat{i}_{ea}, i_{eb}}}{2}, k_{i_{eb}}(t) = \ell \mid Z_{\hat{i}_{ea},1}, \dots, Z_{\hat{i}_{ea},m}\right) \\ &\leq \sum_{\ell=L_{i_{eb}}}^T \Pr\left(\theta_{i_{eb}}^t \geq \frac{S_{i_{eb}}(t)}{k_{i_{eb}}(t)} + \frac{\Delta_{\hat{i}_{ea}, i_{eb}}}{4}, k_{i_{eb}}(t) = \ell \mid Z_{\hat{i}_{ea},1}, \dots, Z_{\hat{i}_{ea},m}\right). \end{aligned} \quad (24)$$

This inequality is due to the definition of event $A_{i_{eb}}(t)$. For any given t , $\theta_{i_{eb}}(t)$ follows $\text{Beta}(\ell\bar{Z}_{i_{eb},\ell} + 1, \ell - \ell\bar{Z}_{i_{eb},\ell} + 1)$, expressed as $W(\ell, \bar{Z}_{i_{eb},\ell})$. Additionally, let $F_{\alpha,\beta}^B(y)$ denote the cumulative distribution function (cdf) of Beta distribution for all positive integers α and β , where y represents the number of successful explorations. It holds that

$$\begin{aligned} & (24) \\ &\leq \sum_{\ell=L_{i_{eb}}}^T \Pr\left(W(\ell, \bar{Z}_{i_{eb},\ell}) > \bar{Z}_{i_{eb},\ell} + \frac{\Delta_{\hat{i}_{ea}, i_{eb}}}{4} \mid Z_{\hat{i}_{ea},1}, \dots, Z_{\hat{i}_{ea},m}\right) \\ &= \sum_{\ell=L_{i_{eb}}}^T \Pr\left(W(\ell, \bar{Z}_{i_{eb},\ell}) > \bar{Z}_{i_{eb},\ell} + \frac{\Delta_{\hat{i}_{ea}, i_{eb}}}{4}\right) \\ &= \sum_{\ell=L_{i_{eb}}}^T \Pr\left(F_{\ell+1, \bar{Z}_{i_{eb},\ell} + \frac{\Delta_{\hat{i}_{ea}, i_{eb}}}{4}}^B(\ell\bar{Z}_{i_{eb},\ell})\right) \\ &\leq \sum_{\ell=L_{i_{eb}}}^T \Pr\left(F_{\ell, \bar{Z}_{i_{eb},\ell} + \frac{\Delta_{\hat{i}_{ea}, i_{eb}}}{4}}^B(\ell\bar{Z}_{i_{eb},\ell})\right) \\ &\leq \sum_{\ell=L_{i_{eb}}}^T \exp\left\{-\frac{2\ell\Delta_{\hat{i}_{ea}, i_{eb}}^2}{16}\right\} \leq \frac{1}{T^2}. \end{aligned} \quad (25)$$

The first inequality arises from the fact that $\bar{Z}_{i_{eb},\ell}$ and $W(\ell, \bar{Z}_{i_{eb},\ell})$ are independent of $Z_{\hat{i}_{ea},d}$ for all $d = 1, \dots, m$. The last equality and the third inequality are derived from the following facts:

$$F_{\alpha,\beta}^B(y) = 1 - F_{\alpha+\beta-1,y}^B(\alpha - 1),$$

and,

$$F_{\alpha+1,\beta}^B(y) \leq (1 - \beta)F_{\alpha,\beta}^B(y) + \beta F_{\alpha,\beta}^B(y) = F_{\alpha,\beta}^B(y),$$

also, the last inequality is due to Chernoff-Hoeffding bounds. Substituting above into (21), we obtain that $\Pr\left(\overline{E_i^+(t, \hat{p})} \mid s(j)\right) \leq \frac{2}{T^2}$. Similarly, we can obtain that $\Pr\left(\overline{E_i^-(t, \hat{p})} \mid s(j)\right) \leq \frac{2}{T^2}$.

Combining two events, we finish the proof.

B. Proof of Theorem 1

In this proof, the core idea is to subdivide the training interval $I(m)$. Define that event $M(t)$ holds at time t , if $\theta_{i_{ea}}^t$ exceeds $\mu_{i_{ea}} + \frac{\Delta_{i_{ea}, i_{eb}}}{2}$, i.e.,

$$M(t) : \theta_{i_{ea}}^t \geq \max_{i_{eb} \in C(t)} \mu_{i_{eb}} + \frac{\Delta_{i_{ea}, i_{eb}}}{2}. \quad (26)$$

In training interval $I(m)$, the event $M(t)$ represents the selection of the client i_{eb} that fails to meet the warm-up rounds condition, i.e., $i_{eb} \notin C(t)$. This occurs because the high-probability event $E(t, \hat{i}_{ea})$ is not easily violated. Namely, the occurrences of event $M(t)$ can divide $I(m)$ into sub-interval $I_m(l)$ with $l = 1, \dots, \gamma_m + 1$, where γ_m denotes the number of occurrences of the event $M(t)$ in training interval $I(m)$.

Next, the number of selection rounds of the client i_{eb} ($i_{eb} \in C(t)$) is at most

$$\sum_{l=1}^{\gamma_m+1} |I_m(l)| + \sum_{t \in I(m)} \mathbb{I}(\overline{E_{i_{eb}}(t, \hat{i}_{ea})}), \quad (27)$$

where $\mathbb{I}(\cdot)$ is the indicator function. To divide sub-interval $I(l)$, the $V_m^{l,g}$ can be defined as follows:

$$V_m^{l,g} = \left| \left\{ t \in I_m(l) : \mu_g = \max_{i_{eb} \in C(t)} \mu_{i_{eb}} \right\} \right|, \quad (28)$$

where the $V_m^{l,g}$ denotes the number of selection rounds in $I_m(l)$, for which a is the best client from $C(t)$. Then, the sub-interval $I_m(l)$ can be covered by the $V_m^{l,g}$, i.e.,

$$|I_m(l)| = \sum_{g \in \mathcal{M}_{N-\bar{p}}} V_m^{l,g}. \quad (29)$$

For the $V_m^{\ell,g}$, the regret of selecting any client i_{eb} ($i_{eb} \in C(t)$) is at most $3\Delta_{\hat{i}_{ea},g} + \mathbb{I}(\overline{E_{i_{eb}}(t, \hat{i}_{ea})})$. The reason is that, if a saturated client i_{eb} is selected at a time t in one of the $V_m^{\ell,g}$, then, $E_{i_{eb}}(t, \hat{i}_{ea})$ is violated, or

$$\mu_{i_{eb}} + \frac{\Delta_{\hat{i}_{ea},i_{eb}}}{2} \geq \theta_{i_{eb}}^t \geq \theta_g^t \geq \mu_g - \frac{\Delta_{\hat{i}_{ea},g}}{2}. \quad (30)$$

The expected regret of train interval $I(m)$ is bounded as follows:

$$\begin{aligned} & \mathbb{E}[\mathcal{R}(I(m))] \\ & \leq \mathbb{E} \left[\sum_{l=1}^{\gamma_m+1} \sum_{g \in \mathcal{M}_{N-\bar{p}}} \sum_{t \in V_m^{l,a}} \left(3\Delta_{\hat{i}_{ea},g} + \mathbb{I}(\overline{E_{i_{eb}}(t, \hat{i}_{ea})}) \right) \right] \\ & + \sum_{t \in I(m)} \mathbb{I}(\overline{E_{i_{eb}}(t, \hat{i}_{ea})}) \\ & = \mathbb{E} \underbrace{\left[\sum_{l=1}^{\gamma_m+1} \sum_{g \in \mathcal{M}_{N-\bar{p}}} 3\Delta_{\hat{i}_{ea},g} V_m^{l,g} \right]}_{A_3} + 2\mathbb{E} \left[\sum_{t \in I(m)} \mathbb{I}(\overline{E_{i_{eb}}(t, \hat{i}_{ea})}) \right]. \end{aligned} \quad (31)$$

For A_3 , it holds that

$$\begin{aligned} & \mathbb{E} \left[\sum_{l=1}^{\gamma_m+1} V_j^{l,g} \mid s_{\hat{i}_{ea}}(m) \right] \\ & = \mathbb{E} \left[\sum_{l=1}^T V_m^{l,g} \cdot \mathbf{I}(\gamma_m \geq l-1) \mid s_{\hat{i}_{ea}}(m) \right]. \end{aligned} \quad (32)$$

Let $\mathcal{F}_{\ell-1}$ denote the historical information, i.e., the values of $\theta_{i_{eb}}^t$ and the outcomes of client selection at round t before the

start of training interval $I_m(l)$. Since the value of the variable $\mathbf{I}(\gamma_j \geq l-1)$ is determined by $\mathcal{F}_{\ell-1}$, we have that

$$\begin{aligned} & (32) \\ & = \mathbb{E} \left[\sum_{l=1}^T \mathbb{E} \left[V_m^{l,g} \cdot \mathbf{I}(\gamma_m \geq l-1) \mid s_{\hat{i}_{ea}}(m), \mathcal{F}_{l-1} \right] \mid s_{\hat{i}_{ea}}(m) \right] \\ & = \mathbb{E} \left[\sum_{l=1}^T \mathbb{E} \left[V_j^{\ell,a} \mid s_{\hat{i}_{ea}}(m), \mathcal{F}_{l-1} \right] \cdot \mathbb{I}(\gamma_m \geq l-1) \mid s_{\hat{i}_{ea}}(m) \right], \end{aligned} \quad (33)$$

where the $V_m^{l,g}$ is the length of an period which ends when $M(t)$ happens or if the irrelevant client other than g becomes the best client, or if we attend total round T . Therefore, the $V_m^{l,g}$ is dominated by $\min\{X(m, s_{\hat{i}_{ea}}(m), \mu_g + \frac{\Delta_{\hat{i}_{ea},g}}{2}), T\}$, where $X(m, s_{\hat{i}_{ea}}(m), \mu_g + \frac{\Delta_{\hat{i}_{ea},g}}{2})$ is defined as the number of trials until a sample from $Beta(s_{\hat{i}_{ea}}(m)+1, m-s_{\hat{i}_{ea}}(m)+1)$ exceeds $\mu_g + \frac{\Delta_{\hat{i}_{ea},g}}{2}$. Then, we obtain that

$$\begin{aligned} & \mathbb{E} [V_m^{l,g} \mid s_{\hat{i}_{ea}}(m), \mathcal{F}_{l-1}] \\ & \leq \mathbb{E} \left[\min \left\{ X \left(m, s_{\hat{i}_{ea}}(m), \mu_g + \frac{\Delta_{\hat{i}_{ea},g}}{2} \right), T \right\} \mid s_{\hat{i}_{ea}}(m) \right]. \end{aligned} \quad (34)$$

Next, we can get that

$$\begin{aligned} & \mathbb{E} \left[\sum_{l=1}^T \mathbb{E} \left[V_j^{\ell,a} \mid s_{\hat{i}_{ea}}(m), \mathcal{F}_{l-1} \right] \cdot \mathbb{I}(\gamma_m \geq l-1) \mid s_{\hat{i}_{ea}}(m) \right] \\ & \leq \mathbb{E} [\mathbb{E} [\gamma_m + 1 \mid s_{\hat{i}_{ea}}(m)]] \\ & \quad \cdot \mathbb{E} \left[\sum_{g \in \mathcal{M}_{N-\bar{p}}} \Delta_{\hat{i}_{ea},g} \mathbb{E} [\min \{C, T\} \mid s_{\hat{i}_{ea}}(m)] \right], \end{aligned} \quad (35)$$

where $C = X \left(m, s_{\hat{i}_{ea}}(m), \mu_g + \frac{\Delta_{\hat{i}_{ea},g}}{2} \right)$.

Combining (31) and (35), we finish the proof.

C. Proof of Lemma 2

As mentioned in (4), we get that

$$\begin{aligned} & \left\| \mathbf{w}_{oe}^{(t)} - \mathbf{w}_o^{(t)} \right\|^2 \\ & = \frac{1}{(|\mathcal{S}_o^t| + |\mathcal{S}_p^t|)^2} \left\| \sum_{i_e \in \mathcal{S}_p^t} \mathbf{w}_{i_e}^t - \sum_{i_e \in \mathcal{S}_p^t} \mathbf{w}_o^{(t)} \right\|^2 \\ & \leq \frac{|\mathcal{S}_p^t|}{(|\mathcal{S}_o^t| + |\mathcal{S}_p^t|)^2} \sum_{i_e \in \mathcal{S}_p^t} \left\| \mathbf{w}_{i_e}^{(t)} - \mathbf{w}_o^{(t)} \right\|^2, \end{aligned} \quad (36)$$

where the last inequality is due to the Cauchy-Swartz and the AM-GM inequalities. In our framework, we hold the inequality that:

$$\left\| \mathbf{w}_{oi_e}^{(t)} - \mathbf{w}_o^{(t)} \right\|^2 \leq \alpha^{(t)}, \forall i_e \in \mathcal{S}_p^t. \quad (37)$$

Due to the equation that $\mathbf{w}_{oi_e}^{(t)} = \frac{\sum_{i_o \in \mathcal{S}_o^t} \mathbf{w}_{i_o}^{(t)} + \varepsilon \mathbf{w}_{i_e}^{(t)}}{|\mathcal{S}_o^t| + \varepsilon}$, we obtain the inequality,

$$\left\| \mathbf{w}_{i_e}^{(t)} - \mathbf{w}_o^{(t)} \right\|^2 \leq \frac{(|\mathcal{S}_o^t| + \varepsilon)^2}{\varepsilon^2} \alpha^{(t)}, \forall i_e \in \mathcal{S}_p^t. \quad (38)$$

Combining (36) and (38), we obtain that,

$$\left\| \mathbf{w}_{oe}^{(t)} - \mathbf{w}_o^{(t)} \right\|^2 \leq \frac{(|\mathcal{S}_o^t| + \varepsilon)^2 |\mathcal{S}_p^t|^2}{(|\mathcal{S}_o^t| + |\mathcal{S}_p^t|)^2 \varepsilon^2} \alpha^{(t)}, \quad (39)$$

where ε is the hyper-parameter to control the aggregation weight for each new participation client, and $\alpha^{(t)}$ is the adaptive threshold that controls the participation of new clients.

D. Proof of Theorem 2

Firstly, we define additional notations for the ease of analysis. The local updating rule is formulated as follows:

$$\mathbf{w}_{i,r+1}^{(t)} = \mathbf{w}_{i,r}^{(t)} - \underbrace{\eta \nabla f_i(\mathbf{w}_{i,r}^{(t)}; \xi_i^t)}_{=g_{i,r}^t}$$

where $w_{i,r}^t$ is the local model of client i under the t -th round and r -th local round; η is the step size; $g_{i,r}^t = \nabla f_i(\mathbf{w}_{i,r}^{(t)}; \xi_i^t)$ is the stochastic gradient over mini-batch ξ_i^t ; R is the total number of local rounds, when local round r is equal to R , one local updating is completed. Suppose that $g_{i,r}^t$ is the unbiased estimate of $\nabla f_i(\mathbf{w}_{i,r}^{(t)})$, i.e., $\mathbb{E}[g_{i,r}^t] = \nabla f_i(\mathbf{w}_{i,r}^{(t)})$. We also rewrite the global updating rule as follows:

$$\mathbf{w}_{oe}^{(t+1)} = \mathbf{w}_{oe}^{(t)} - \underbrace{\eta R \sum_{i \in \mathcal{S}^t} \sum_{r=0}^{R-1} g_{i,r}^t}_{=\tilde{\eta} g_t} \quad (40)$$

where $\mathbf{w}_{oe}^{(t)}$ is the global model at round t ; \mathcal{S}^t represents the selected clients with $S = |\mathcal{S}^t|$; $\tilde{\eta}$ and g_t can be considered as the step size and approximate stochastic gradient for the global model, respectively. We consider the expectation inequality as follows:

$$\begin{aligned} & \mathbb{E} [F(\mathbf{w}_{oe}^{(t+1)}) - F(\mathbf{w}_{oe}^{(t)})] \\ & \leq \mathbb{E} [\langle \nabla F(\mathbf{w}_{oe}^{(t)}), \mathbf{w}_{oe}^{(t+1)} - \mathbf{w}_{oe}^{(t)} \rangle] \\ & + \frac{L_p}{2} \mathbb{E} \left\| \mathbf{w}_{oe}^{(t+1)} - \mathbf{w}_{oe}^{(t)} \right\|^2 \\ & \leq -\tilde{\eta} \mathbb{E} \left\| \nabla F(\mathbf{w}_{oe}^{(t)}) \right\|^2 + \frac{\tilde{\eta}}{2} \mathbb{E} \left\| g_t - \nabla F(\mathbf{w}_{oe}^{(t)}) \right\|^2 \quad (41) \\ & + \frac{\tilde{\eta}}{2} \mathbb{E} \left\| \nabla F(\mathbf{w}_{oe}^{(t)}) \right\|^2 + \frac{L_p \tilde{\eta}^2}{2} \mathbb{E} \|g_t\|^2 \\ & = \frac{\tilde{\eta}}{2} \left\| \frac{1}{S} \sum_{i \in \mathcal{S}^t} \nabla f_i(\mathbf{w}_{oe}^{(t)}) - \nabla F(\mathbf{w}_{oe}^{(t)}) \right\|^2 \\ & - \frac{\tilde{\eta}}{2} \mathbb{E} \left\| \nabla F(\mathbf{w}_{oe}^{(t)}) \right\|^2 + \frac{L_p \tilde{\eta}^2}{2} \mathbb{E} \|g_t\|^2, \end{aligned}$$

where the first inequality is due to the L_p -smoothness assumption, the sampling set $\mathcal{S}^t = \mathcal{S}_o^t \cup \mathcal{S}_p^t$ with $S = |\mathcal{S}_o^t| + |\mathcal{S}_p^t|$, and the last inequality is based on the Cauchy-Swartz and

the AM-GM inequalities. Then, the last term is bounded as follows:

$$\begin{aligned} & \mathbb{E} \|g_t\|^2 \\ & = \mathbb{E} \left\| \frac{1}{SR} \sum_{k,r}^{S^t,R} g_{i,r}^t \right\|^2 \\ & \leq 3 \mathbb{E} \left\| \frac{1}{SR} \sum_{k,r}^{S^t,R} g_{i,r}^t - \frac{1}{S} \sum_{i \in \mathcal{S}^t} \nabla f_i(\mathbf{w}_{oe}^{(t)}) \right\|^2 \\ & + 3 \mathbb{E} \left\| \nabla F(\mathbf{w}_{oe}^{(t)}) \right\|^2 \\ & + 3 \mathbb{E} \left\| \frac{1}{S} \sum_{i \in \mathcal{S}^t} \nabla f_i(\mathbf{w}_{oe}^{(t)}) - \nabla F(\mathbf{w}_{oe}^{(t)}) \right\|^2 \quad (42) \\ & \leq \frac{3}{NR} \sum_{k,r}^{N,R} \|g_{i,r}^t - \nabla f_i(\mathbf{w}_{oe}^{(t)})\|^2 \\ & + 3 \mathbb{E} \left\| \nabla F(\mathbf{w}_{oe}^{(t)}) \right\|^2 \\ & + 3 \mathbb{E} \left\| \frac{1}{S} \sum_{i \in \mathcal{S}^t} \nabla f_i(\mathbf{w}_{oe}^{(t)}) - \nabla F(\mathbf{w}_{oe}^{(t)}) \right\|^2, \end{aligned}$$

where the first inequality is due to the Cauchy-Swartz and the AM-GM inequalities and the second inequality follows from

$$\begin{aligned} & \mathbb{E} \left\| \frac{1}{SR} \sum_{i,r}^{S^t,R} g_{i,r}^t - \frac{1}{S} \sum_{i \in \mathcal{S}^t} \nabla f_i(\mathbf{w}_{oe}^{(t)}) \right\|^2 \\ & \leq \frac{1}{SR} \mathbb{E} \sum_{k,r}^{S^t,R} \|g_{i,r}^t - \nabla f_i(\mathbf{w}_{oe}^{(t)})\|^2 \quad (43) \\ & = \frac{1}{SR} \sum_{i,r}^{N,R} \|g_{i,r}^t - \nabla f_k(\mathbf{w}_{oe}^{(t)})\|^2 \mathbb{E}_{\mathcal{S}^t} [\mathbb{I}_{i \in \mathcal{S}^t}] \\ & = \frac{1}{NR} \sum_{i,r}^{N,R} \|g_{i,r}^t - \nabla f_i(\mathbf{w}_{oe}^{(t)})\|^2, \end{aligned}$$

where N is equal to $N_o + N_e$, and $\mathbb{I}_{i \in \mathcal{S}^t}$ is the indicator function with $\mathbb{E}[\mathbb{I}_{i \in \mathcal{S}^t}] = \frac{S}{N}$.

Substituting (42) and (43) to (41), we get that

$$\begin{aligned} & \mathbb{E} [F(\mathbf{w}_{oe}^{(t+1)}) - F(\mathbf{w}_{oe}^{(t)})] \\ & \leq -\frac{\tilde{\eta}(1-3L_p\tilde{\eta})}{2} \mathbb{E} \left\| \nabla F(\mathbf{w}_{oe}^{(t)}) \right\|^2 \\ & + \frac{3L_p\tilde{\eta}^2}{2} \underbrace{\mathbb{E} \left\| \frac{1}{S} \sum_{i \in \mathcal{S}^t} \nabla f_i(\mathbf{w}_{oe}^{(t)}) - \nabla F(\mathbf{w}_{oe}^{(t)}) \right\|^2}_{A_4} \quad (44) \\ & + \frac{\tilde{\eta}(1+3L_p\tilde{\eta})}{2} \frac{1}{NR} \sum_{i,r}^{N,R} \underbrace{\mathbb{E} \left\| g_{i,r}^t - \nabla f_i(\mathbf{w}_{oe}^{(t)}) \right\|^2}_{A_5}. \end{aligned}$$

For the A_4 , we obtain the following equality:

$$\begin{aligned} & \mathbb{E} \left\| \frac{1}{S} \sum_{i \in \mathcal{S}^t} \nabla f_i \left(\mathbf{w}_{oe}^{(t)} \right) - \nabla F \left(\mathbf{w}_{oe}^{(t)} \right) \right\|^2 \\ &= \frac{1}{S^2} \mathbb{E} \left\| \sum_{i=1}^N \mathbb{I}_{i \in \mathcal{S}^t} \left(\nabla f_i \left(\mathbf{w}_{oe}^{(t)} \right) - \nabla F \left(\mathbf{w}_{oe}^{(t)} \right) \right) \right\|^2 \\ &= \frac{1}{S^2} \sum_{i=1}^N \mathbb{E} [\mathbb{I}_{i \in \mathcal{S}^t}] \left\| \nabla f_i \left(\mathbf{w}_{oe}^{(t)} \right) - \nabla F \left(\mathbf{w}_{oe}^{(t)} \right) \right\|^2 \\ &+ \frac{1}{S^2} \sum_{i_1 \neq i_2} \mathbb{E} [\mathbb{I}_{i_1 \in \mathcal{S}^t} \mathbb{I}_{i_2 \in \mathcal{S}^t}] \\ &\quad \left\langle \nabla f_{i_1} \left(\mathbf{w}_{oe}^{(t)} \right) - \nabla F \left(\mathbf{w}_{oe}^{(t)} \right), \nabla f_{i_2} \left(\mathbf{w}_{oe}^{(t)} \right) - \nabla F \left(\mathbf{w}_{oe}^{(t)} \right) \right\rangle. \end{aligned} \quad (45)$$

According to

$$\begin{aligned} & \sum_{i=1}^N \left\| \nabla f_i \left(\mathbf{w}_{oe}^{(t)} \right) - \nabla F \left(\mathbf{w}_{oe}^{(t)} \right) \right\|^2 \\ &+ \left\langle \nabla f_{i_1} \left(\mathbf{w}_{oe}^{(t)} \right) - \nabla F \left(\mathbf{w}_{oe}^{(t)} \right), \nabla f_{i_2} \left(\mathbf{w}_{oe}^{(t)} \right) - \nabla F \left(\mathbf{w}_{oe}^{(t)} \right) \right\rangle \\ &= 0, \end{aligned}$$

and $\mathbb{E}_{\mathcal{S}^t} [\mathbb{I}_{i_1 \in \mathcal{S}^t} \mathbb{I}_{i_2 \in \mathcal{S}^t}] = \frac{S(S-1)}{N(N-1)}$ with $i_1 \neq i_2$. We bound (45) as follows:

$$\begin{aligned} & \mathbb{E}_{\mathcal{S}^t} \left\| \frac{1}{S} \sum_{i \in \mathcal{S}^t} \nabla f_i \left(\mathbf{w}_{oe}^{(t)} \right) - \nabla F \left(\mathbf{w}_{oe}^{(t)} \right) \right\|^2 \\ & \leq \frac{N/S-1}{N-1} \sum_{i=1}^N \frac{1}{N} \left\| \nabla f_i \left(\mathbf{w}_{oe}^{(t)} \right) - \nabla F \left(\mathbf{w}_{oe}^{(t)} \right) \right\|^2. \end{aligned} \quad (46)$$

The A_5 is bounded as follows:

$$\begin{aligned} \mathbb{E} \left\| g_{i,r}^t - \nabla f_i \left(\mathbf{w}_{oe}^{(t)} \right) \right\|^2 &= \mathbb{E} \left\| \nabla f_i \left(\mathbf{w}_{i,r}^{(t)} \right) - \nabla f_i \left(\mathbf{w}_{oe}^{(t)} \right) \right\|^2 \\ &\leq L_p \mathbb{E} \left\| \mathbf{w}_{i,r}^{(t)} - \mathbf{w}_{oe}^{(t)} \right\|^2, \end{aligned} \quad (47)$$

where the inequality is due to the L_p -smoothness assumption. We further bound (47) as follows:

$$\begin{aligned} & \mathbb{E} \left\| \mathbf{w}_{i,r}^{(t)} - \mathbf{w}_{oe}^{(t)} \right\|^2 = \mathbb{E} \left\| \mathbf{w}_{i,r-1}^{(t)} - \mathbf{w}_{oe}^{(t)} - \eta g_{i,r-1}^t \right\|^2 \\ & \leq 2 \mathbb{E} \left\| \mathbf{w}_{i,r-1}^{(t)} - \mathbf{w}_{oe}^{(t)} - \eta \nabla f_i \left(\mathbf{w}_{oe}^{(t)} \right) \right\|^2 \\ & \quad + 2\eta^2 \mathbb{E} \left\| g_{i,r-1}^t - \nabla f_i \left(\mathbf{w}_{oe}^{(t)} \right) \right\|^2 \\ & \leq 2 \left(1 + \frac{1}{2R} + L_p^2 \eta^2 \right) \mathbb{E} \left\| \mathbf{w}_{i,r-1}^{(t)} - \mathbf{w}_{oe}^{(t)} \right\|^2 \\ & \quad + 2(1+2R)\eta^2 \mathbb{E} \left\| \nabla f_i \left(\mathbf{w}_{oe}^{(t)} \right) \right\|^2, \end{aligned} \quad (48)$$

Next, unrolling (48) and utilizing the fact that $L_p^2 \eta^2 = L_p^2 \frac{\tilde{\eta}^2}{R^2} \leq \frac{1}{4R^2} \leq \frac{1}{2R}$ for $\tilde{\eta} \leq \frac{1}{2L_p}$, and that $2(1+2R)\eta^2 =$

$2(1+2R) \frac{\tilde{\eta}^2}{R^2} \leq \frac{6\tilde{\eta}^2}{R}$, we obtain the following results:

$$\begin{aligned} & \mathbb{E} \left\| \mathbf{w}_{i,r}^{(t)} - \mathbf{w}_{oe}^{(t)} \right\|^2 \\ & \leq \frac{6\tilde{\eta}^2}{R} \mathbb{E} \left\| \nabla f_i \left(\mathbf{w}_{oe}^{(t)} \right) \right\|^2 \sum_{r=0}^{R-1} 2 \left(1 + \frac{1}{R} \right)^r \\ & \leq \frac{24\tilde{\eta}^2 \ln(1+1/R)}{R} \mathbb{E} \left\| \nabla f_i \left(\mathbf{w}_{oe}^{(t)} \right) \right\|^2. \end{aligned} \quad (49)$$

Substituting (47) and (49) to (44), we get that

$$\begin{aligned} & \mathbb{E} \left[F \left(\mathbf{w}_{oe}^{(t+1)} \right) - F \left(\mathbf{w}_{oe}^{(t)} \right) \right] \\ & \leq -\frac{\tilde{\eta}(1-3L_p\tilde{\eta})}{2} \mathbb{E} \left\| \nabla F \left(\mathbf{w}_{oe}^{(t)} \right) \right\|^2 \\ & \quad + \frac{3L_p\tilde{\eta}^2}{2} \frac{N/S-1}{N-1} \sum_{i=1}^N \frac{1}{N} \mathbb{E} \left\| \nabla f_i \left(\mathbf{w}_{oe}^{(t)} \right) - \nabla F \left(\mathbf{w}_{oe}^{(t)} \right) \right\|^2 \\ & \quad + \frac{\tilde{\eta}(1+3L_p\tilde{\eta})}{2} \frac{8L_p^2\tilde{\eta}^2 \ln(1+1/R)}{R} \\ & \quad (3 \sum_{i=1}^N \frac{1}{N} \mathbb{E} \left\| \nabla f_i \left(\mathbf{w}_{oe}^{(t)} \right) - \nabla F \left(\mathbf{w}_{oe}^{(t)} \right) \right\|^2 + 3 \mathbb{E} \left\| \nabla F \left(\mathbf{w}_{oe}^{(t)} \right) \right\|^2), \end{aligned} \quad (50)$$

where the inequality is using the fact that $\mathbb{E} [\|X\|^2] = \mathbb{E} [\|X - \mathbb{E}[X]\|^2] + \mathbb{E}[\|X\|]^2$.

Re-considering (41), we can get that

$$\begin{aligned} & \mathbb{E} \left[F \left(\mathbf{w}^{(t+1)} \right) - F \left(\mathbf{w}^{(t)} \right) \right] \\ & \leq -\frac{\tilde{\eta}}{4} \mathbb{E} \left\| \nabla F \left(\mathbf{w}_{oe}^{(t)} \right) \right\|^2 + CL_p \max_{i \in \mathcal{I}} \{\sigma_{F,i}^2\} \tilde{\eta}^2, \end{aligned} \quad (51)$$

where $C = \frac{3L(N/S-1)}{2(N-1)} + \frac{15L \ln(1+1/R)}{R}$, and $\max_{i \in \mathcal{I}} \{\sigma_{F,i}^2\}$ represents the largest client's variance. This inequality is due to the fact that

$$\frac{1}{2} - L_p \tilde{\eta} \left(\frac{3}{2} + \frac{15 \ln(1+1/R)}{R} \right) \geq \frac{1}{4} \quad (52)$$

with the condition that

$$\tilde{\eta} \leq \frac{1}{\left(6 + \frac{60 \ln(1+1/R)}{R} \right) L_p} \leq \frac{1}{2L_p}.$$

Re-arranging (51) and telescoping, we get that

$$\begin{aligned} \frac{1}{T} \sum_{t=1}^T \mathbb{E} \left\| \nabla F \left(\mathbf{w}_{oe}^{(t)} \right) \right\|^2 & \leq \frac{\mathbb{E} \left[F \left(\mathbf{w}_{oe}^{(t_0)} \right) - F \left(\mathbf{w}_{oe}^{(T)} \right) \right]}{\tilde{\eta} T} \\ & \quad + CL_p \max_{i \in \mathcal{I}} \{\sigma_{F,i}^2\} \tilde{\eta}, \end{aligned} \quad (53)$$

where t_0 is the insertion time. Suppose that \mathbf{w}_{oe}^* is the unique solution for the global loss. Defining $\Delta_{F,t_0} = F \left(\mathbf{w}_{oe}^{(t_0)} \right) - F \left(\mathbf{w}_{oe}^* \right)$, we get that

$$\frac{1}{T} \sum_{t=1}^T \mathbb{E} \left\| \nabla F \left(\mathbf{w}_{oe}^{(t)} \right) \right\|^2 \leq \frac{\Delta_{F,t_0}}{\tilde{\eta} T} + CL_p \max_{i \in \mathcal{I}} \{\sigma_{F,i}^2\} \tilde{\eta}. \quad (54)$$

Next, we bound $\Delta_{F_{t_0}}$ as follows:

$$\begin{aligned} & F\left(\mathbf{w}_{oe}^{(t_0)}\right) - F\left(\mathbf{w}_{oe}^*\right) \\ & \leq \left\langle \nabla F\left(\mathbf{w}_{oe}^*\right), \mathbf{w}_{oe}^{(t_0)} - \mathbf{w}_{oe}^* \right\rangle + \frac{L_p}{2} \left\| \mathbf{w}_{oe}^{(t_0)} - \mathbf{w}_{oe}^* \right\|^2 \quad (55) \\ & = \frac{L_p}{2} \left\| \mathbf{w}_{oe}^{(t_0)} - \mathbf{w}_{oe}^* \right\|^2. \end{aligned}$$

This inequality is due to the L_p -smoothness assumption and the fact that \mathbf{w}_{oe}^* is the unique solution. Here, the $\left\| \mathbf{w}_{oe}^{(t_0)} - \mathbf{w}_{oe}^* \right\|^2$ can be further bounded as follows:

$$\begin{aligned} & \left\| \mathbf{w}_{oe}^{(t_0)} - \mathbf{w}_{oe}^* \right\|^2 \\ & \leq \underbrace{3 \left\| \mathbf{w}_{oe}^{(t_0)} - \mathbf{w}_o^{(t_0)} \right\|^2}_{\text{Participating client diversity}} + \underbrace{3 \left\| \mathbf{w}_{oe}^* - \mathbf{w}_o^* \right\|^2}_{\text{Participating client diversity}} \quad (56) \\ & + \underbrace{3 \left\| \mathbf{w}_o^{(t_0)} - \mathbf{w}_o^* \right\|^2}_{\text{No client participation diversity}}, \end{aligned}$$

where the $\left\| \mathbf{w}_o^{(t_0)} - \mathbf{w}_o^* \right\|^2$ represents the model process under no-client participation scenario, and the $\left\| \mathbf{w}_{oe}^{(t_0)} - \mathbf{w}_o^{(t_0)} \right\|^2$ is the diversity between two scenarios.

Using the Lemma 2, the $\left\| \mathbf{w}_{oe}^* - \mathbf{w}_o^* \right\|^2$ is bounded as follows:

$$\left\| \mathbf{w}_{oe}^* - \mathbf{w}_o^* \right\|^2 \leq \frac{\left(|\mathcal{S}_o^{T^*}| + \varepsilon \right)^2 |\mathcal{S}_p^{T^*}|^2}{\left(|\mathcal{S}_o^{T^*}| + |\mathcal{S}_e^{T^*}| \right)^2 \varepsilon^2} \alpha^{(T^*)}, \quad (57)$$

where T^* is specific training round corresponding to \mathbf{w}_{oe}^* . Considering a fixed client selection size over training process, we get that

$$\begin{aligned} & \left\| \mathbf{w}_{oe}^{(t_0)} - \mathbf{w}_{oe}^* \right\|^2 \\ & \leq \frac{3(|\mathcal{S}_o| + \varepsilon)^2 |\mathcal{S}_p|^2}{(|\mathcal{S}_o| + |\mathcal{S}_e|)^2 \varepsilon^2} \left(\alpha^{(t_0)} + \alpha^{(T^*)} \right) + 3 \left\| \mathbf{w}_o^{(t_0)} - \mathbf{w}_o^* \right\|^2. \quad (58) \end{aligned}$$

Combing (54), (55) and (58), we finish the proof.

E. The Public Parameters of Our Framework

Here, we present the public parameters of the Fed-TS framework. For the CIFAR-10, Fashion-MNIST, and AG-news datasets, the parameters are summarized as follows:

- CIFAR-10 dataset:** total round $T = 100$, local epoch $E = 3$, local batch size $B = 200$, learning rate $\eta = 0.02$, client participation rate P_o for group \mathcal{I}_o equals 0.5.
- Fashion-MNIST dataset:** total round $T = 100$, local epoch $E = 3$, local batch size $B = 300$, learning rate $\eta = 0.03$, client participation rate P_o for group \mathcal{I}_o equals 0.5.
- AG-news dataset:** total round $T = 100$, local epoch $E = 2$, local batch size $B = 400$, learning rate $\eta = 0.03$, client participation rate P_o for group \mathcal{I}_o equals 0.5.

REFERENCES

- H. B. Zhang, H. L. Zhang, B. Di, and L. Y. Song, "Holographic integrated sensing and communications: principles, technology, and implementation," *IEEE Commun Mag.*, vol. 61, no. 5, pp. 83-89, 2023.
- C. Zhang, Y. Xie, H. Bai, B. Yu, W. H. Li, and Y. Gao, "A survey on federated learning," *Knowledge-Based Syst.*, vol. 216, pp. 106775, 2021.
- D. Chai, L. Wang, L. Yang, J. Zhang, K. Chen, and Q. Yang, "A survey for federated learning evaluations: goals and measures," *IEEE Trans. Knowl. Data Eng.*, vol. 36, no. 10, pp. 5007-5024, 2024.
- S. M. Azimi-Abarghouyi and V. Fodor, "Scalable hierarchical over-the-air federated learning," *IEEE Trans. Wirel. Commun.*, vol. 23, no. 8, pp. 8480-8496, 2024.
- X. Huang, P. Li, H. Du, J. Kang, D. Niyato, D. I. Kim, and Y. Wu, "Federated learning-empowered ai-generated content in wireless networks," *IEEE Netw.*, vol. 38, no. 5, pp. 304-313, 2024.
- A. Imteaj, U. Thakker, S. Wang, J. Li, and M. H. Amini, "A survey on federated learning for resource-constrained IoT devices," *IEEE Internet Things J.*, vol. 9, no. 1, pp. 1-24, 2022.
- F. Foukalas and A. Tziouvaras, "Federated learning protocols for IoT edge computing," *IEEE Internet Things J.*, vol. 9, no. 15, pp. 13570-13581, 2022.
- H. Mun, K. Han, H. K. Yeun, E. Damiani, D. Puthal, T.-Y. Kim, and C. Y. Yeun, "Emerging blockchain and reputation management in federated learning: Enhanced security and reliability for Internet of Vehicles (IoV)," *IEEE Trans. Veh. Technol.*, vol. 74, no. 2, pp. 1893-1908, 2025.
- L. Nagalapatti and R. Narayanan, "Game of gradients: Mitigating irrelevant clients in federated learning," in *Proc. AAAI Conf. Artif. Intell.*, vol. 35, 2021, pp. 9046-9054.
- M. Yang, H. Qian, X. Wang, Y. Zhou, and H. Zhu, "Client selection for federated learning with label noise," *IEEE Trans. Veh. Technol.*, vol. 71, no. 2, pp. 2193-2197, 2022.
- J. Fan, G. Tang, K. Wu, Z. Zhao, Y. Zhou, and S. Huang, "Score-VAE: Root cause analysis for federated-learning-based IoT anomaly detection," *IEEE Internet Things J.*, vol. 11, no. 1, pp. 1041-1053, 2024.
- M. Ma, C. Gong, L. Zeng, Y. Yang, and L. Wu, "FloCOff: Data heterogeneity resilient federated learning with communication-efficient edge offloading," *IEEE J. Sel. Areas Commun.*, vol. 42, no. 11, pp. 3262-3277, 2024.
- T. Li, A. K. Sahu, M. Zaheer, M. Sanjabi, A. Talwalkar, and V. Smith, "Federated optimization in heterogeneous networks," in *Proc. 3rd Conf. Machine Learning and Systems (MLSys)*, 2020, pp. 1-22.
- X. Li, M. Jiang, X. Zhang, M. Kamp, and Q. Dou, "FedBN: Federated learning on non-iid features via local batch normalization," in *Proc. 9th Int. Conf. Learning Representations (ICLR)*, 2021, pp. 1-27.
- D. A. E. Acar, Y. Zhao, R. M. Navarro, M. Mattina, P. N. Whatmough, and V. Saligrama, "Federated learning based on dynamic regularization," in *Proc. 9th Int. Conf. Learning Representations (ICLR)*, 2021, pp. 1-43.
- S. P. Karimireddy, S. Kale, M. Mohri, S. J. Reddi, S. U. Stich, and A. T. Suresh, "Scaffold: Stochastic controlled averaging for federated learning," in *Proc. 37th Int. Conf. Machine Learning (ICML)*, 2020, pp. 5132-5143.
- Z. Zhu, J. Hong, and J. Zhou, "Data-free knowledge distillation for heterogeneous federated learning," in *Proc. 38th Int. Conf. Mach. Learn. (ICML)*, 2021, pp. 12878-12889.
- Q. Li, B. He, and D. Song, "Model-contrastive federated learning," in *Proc. CVPR*, 2021, pp. 10713-10722.
- L. Lan, J. Wang, Z. Li, K. Kant, and W. Liu, "Fedrem: Guided federated learning in the presence of dynamic device unpredictability," *IEEE Trans. Parallel Distributed Syst.*, vol. 35, no. 7, pp. 1189-1206, 2024.
- H. Peng, Y. Yu, and S. Yu, "Re-thinking the effectiveness of batch normalization and beyond," *IEEE Trans. Pattern Anal. Mach. Intell.*, vol. 46, no. 1, pp. 465-478, 2024.
- J. Li, H. Feng, and X. Zhuang, "Convolutional neural networks for spherical signal processing via area-regular spherical haar tight framelets," *IEEE Trans. Neural Networks Learn. Syst.*, vol. 35, no. 4, pp. 4400-4410, 2024.
- F. Xia and W. Cheng, "A survey on privacy-preserving federated learning against poisoning attacks," *Clust. Comput.*, vol. 27, no. 10, pp. 13565-13582, 2024.
- Y. Li, X. Wang, and L. An, "Hierarchical clustering-based personalized federated learning for robust and fair human activity recognition," in *Proc. ACM IMWUT*, vol. 7, no. 1, 2023, pp. 1-38.
- B. McMahan, E. Moore, D. Ramage, S. Hampson, and B. Agüera y Arcas, "Communication-efficient learning of deep networks from decentralized data," in *Proc. 20th Int. Conf. Artif. Intell. Stat. (AISTATS)*, 2017, pp. 1273-1282.

- [25] Y. J. Cho, J. Wang, and G. Joshi, "Client selection in federated learning: Convergence analysis and power-of-choice selection strategies," 2020, arXiv:2010.01243.
- [26] H. Wu and P. Wang, "Node selection toward faster convergence for federated learning on non-iid data," *IEEE Trans. Netw. Sci. Eng.*, vol. 9, no. 5, pp. 3099-3111, 2022.
- [27] H. Ko, J. Lee, S. Seo, S. Pack, and V. C. M. Leung, "Joint client selection and bandwidth allocation algorithm for federated learning," *IEEE Trans. Mob. Comput.*, vol. 22, no. 6, pp. 3380-3390, 2023.
- [28] Y. Xu, Z. Jiang, H. Xu, Z. Wang, C. Qian, and C. Qiao, "Federated learning with client selection and gradient compression in heterogeneous edge systems," *IEEE Trans. Mob. Comput.*, vol. 23, no. 5, pp. 5446-5461, 2024.
- [29] W. Chen, Y. Wang, and Y. Yuan, "Combinatorial multi-armed bandit: General framework and applications," in *Proc. 30th Int. Conf. Mach. Learn. (ICML)*, 2013, pp. 151-159.
- [30] C. Shi and C. Shen, "Federated multi-armed bandits," in *Proc. AAAI Conf. Artif. Intell.*, 2021, pp. 9603-9611.
- [31] T. Huang, W. Lin, W. Wu, L. He, K. Li, and A. Y. Zomaya, "An efficiency-boosting client selection scheme for federated learning with fairness guarantee," *IEEE Trans. Parallel Distributed Syst.*, vol. 32, no. 7, pp. 1552-1564, 2021.
- [32] C. Wu, Y. Zhu, R. Zhang, Y. Chen, F. Wang, and S. Cui, "FedAB: Truthful federated learning with auction-based combinatorial multi-armed bandit," *IEEE Internet Things J.*, vol. 10, no. 17, pp. 15159-15170, 2023.
- [33] D. Russo and B. Van Roy, "An information-theoretic analysis of Thompson sampling," *Journal of Machine Learning Research*, vol. 17, no. 68, pp. 1-30, 2016.
- [34] S. J. Reddi, Z. Charles, M. Zaheer, Z. Garrett, K. Rush, J. Konečný, S. Kumar, and H. B. McMahan, "Adaptive federated optimization," in *Proc. 9th Int. Conf. Learn. Represent. (ICLR)*, 2021, pp. 1-38.
- [35] Z. Lian, J. Cao, Z. Zhu, X. Zhou, and W. Liu, "GOFL: An accurate and efficient federated learning framework based on gradient optimization in heterogeneous IoT systems," *IEEE Internet Things J.*, vol. 11, no. 7, pp. 12459-12474, 2023.
- [36] S. Li, E. C.-H. Ngai, and T. Voigt, "An experimental study of byzantine-robust aggregation schemes in federated learning," *IEEE Trans. Big Data*, vol. 2023, no. 1, pp. 975-988, 2023.
- [37] P. Blanchard, E. El Mhamdi, R. Guerraoui, and J. Stainer, "Machine learning with adversaries: Byzantine tolerant gradient descent," in *Proc. Adv. Neural Inf. Process. Syst.*, 2017, pp. 119-129.
- [38] D. Yin, Y. Chen, R. Kannan, and P. Bartlett, "Byzantine-robust distributed learning: Towards optimal statistical rates," in *Proc. Int. Conf. Mach. Learn.*, pp. 5650-5659, 2018.
- [39] C. Dong, J. Weng, M. Li, J.-N. Liu, Z. Liu, Y. Cheng, and S. Yu, "Privacy-preserving and byzantine-robust federated learning," *IEEE Trans. Dependable Secure Comput.*, vol. 21, no. 2, pp. 889-904, 2024.
- [40] H. Huang, H. Yang, Y. Chen, J. Ye, and D. Wu, "FedRTS: Federated robust pruning via combinatorial thompson sampling," 2025, arXiv:2501.19122.
- [41] D. Yao, S. Li, Y. Xue, and J. Liu, "Constructing adversarial examples for vertical federated learning: optimal client corruption through multi-armed bandit," in *Proc. 12th Int. Conf. Learn. Represent.*, 2024, pp. 1-23.
- [42] Z. Dai, B. K. H. Low, and P. Jaillet, "Federated Bayesian optimization via thompson sampling," in *Proc. 33rd Adv. Neural Inf. Process. Syst. (NeurIPS)*, 2020, pp. 9687-9699.
- [43] J. Komiyama, J. Honda, and H. Nakagawa, "Optimal regret analysis of Thompson sampling in stochastic multi-armed bandit problem with multiple plays," in *Proc. 32nd Int. Conf. Mach. Learn. (ICML)*, pp. 1152-1161.
- [44] S. Wang and W. Chen, "Thompson sampling for combinatorial semi-bandits," in *Proc. 35th Int. Conf. Mach. Learn. (ICML)*, 2018, pp. 5101-5109.
- [45] D. Li, S. Zhou, T. Zeng, and R. H. Chan, "Multi-prototypes convex merging based k-means clustering algorithm," *IEEE Trans. Knowl. Data Eng.*, vol. 36, no. 11, pp. 6653-6666, 2024.
- [46] S. Agrawal and N. Goyal, "Analysis of thompson sampling for the multi-armed bandit problem," in *Proc. 25th Ann. Conf. Learn. Theory (COLT)*, 2012, pp. 39.1-39.26.
- [47] D. Yao, S. Li, Y. Xue, and J. Liu, "Constructing adversarial examples for vertical federated learning: optimal client corruption through multi-armed bandit," in *Proc. 12th Int. Conf. on Learning Representations (ICLR)*, 2024, pp. 1-23.
- [48] X. Li, K. Huang, W. Yang, S. Wang, and Z. Zhang, "On the convergence of fedAvg on Non-IID data," in *Proc. 8th Int. Conf. Learn. Representations (ICLR)*, 2020, pp. 1-26.
- [49] J. Scott, H. Zakerinia, and C. H. Lampert, "PeFLL: personalized federated learning by learning to learn," in *Proc. 20-th Int. Conf. Learn. Representations (ICLR)*, 2024, pp. 1-32.
- [50] X. Su, Y. Zhou, L. Cui, Q. Z. Sheng, Y. Wang, and S. Guo, "Fast-convergent wireless federated learning: A voting based TopK model compression approach," *IEEE J. Sel. Areas Commun.*, vol. 42, no. 11, pp. 3048-3063, 2024.
- [51] H. Chen and H. Vikalo, "Heterogeneity-Guided client sampling: towards fast and efficient Non-IID federated learning," in *Proc. 38th Annual Conference on Neural Information Processing Systems (NeurIPS)*, 2024, pp. 65525-65561.
- [52] Y. Zhou, Q. Ye, and J. Lv, "Communication-efficient federated learning with compensated overlap-FedAvg," *IEEE Trans. Parallel Distrib. Syst.*, vol. 33, no. 1, pp. 192-205, 2022.
- [53] X. Shen, Y. Liu, F. Li, and C. Li, "Privacy-preserving federated learning against label-flipping attacks on non-IID data," *IEEE Internet Things J.*, vol. 11, no. 1, pp. 1241-1255, 2024.
- [54] R. Jin, J. Hu, G. Min, and J. Mills, "Lightweight blockchain-empowered secure and efficient federated edge learning," *IEEE Trans. Comput.*, vol. 72, no. 11, pp. 3314-3325, 2023.
- [55] Q. Li, Y. Diao, Q. Chen, and B. He, "Federated learning on non-iid data silos: An experimental study," in *Proc. 38th IEEE Int. Conf. on Data Engineering (ICDE)*, 2022, pp. 965-978.
- [56] S. Q. Zhang, J. Lin, and Q. Zhang, "A multi-agent reinforcement learning approach for efficient client selection in federated learning," in *Proc. AAAI Conf. Artif. Intell.*, 2022, pp. 9091-9099.
- [57] F. Lai, X. Zhu, H. V. Madhyastha, and M. Chowdhury, "Oort: Efficient federated learning via guided participant selection," in *Proc. 15th USENIX Symp. Operating Syst. Des. Implement. (OSDI)*, 2021, pp. 19-35.
- [58] Z. Ma, Y. Lai, W. B. Kleijn, Y.-Z. Song, L. Wang, and J. Guo, "Variational bayesian learning for dirichlet process mixture of inverted dirichlet distributions in non-gaussian image feature modeling," *IEEE Trans. Neural Networks Learn. Syst.*, vol. 30, no. 2, pp. 449-463, 2019.
- [59] Z. Chen, Z. Huang, J. Zhang, H. Cheng, and J. Li, "Resource allocation and collaborative offloading in multi-UAV-assisted IoV with federated deep reinforcement learning," *IEEE Internet Things J.*, vol. 12, no. 5, pp. 4629-4640, 2025.
- [60] T. Liu, L. Fang, Y. Zhu, W. Tong, and Y. Yang, "A near-optimal approach for online task offloading and resource allocation in edge-cloud orchestrated computing," *IEEE Trans. Mobile Comput.*, vol. 21, no. 8, pp. 2687-2700, 2020.